HEAT REMOVAL ANALYSIS USING NTU/ MICROSCOPIC THEORY AND EXPERIMENTAL FLUID TESTING OF RADAITORS, PUMPS AND FANS FOR THE THERMAL MANAGEMENT SYSTEM OF FORMULA SAE ELECTRIC RACECAR

by

SHAHZAD SHAHRUKH BULSARA

Presented to the Faculty of the Graduate School of

The University of Texas at Arlington in Partial Fulfillment

of the Requirements

for the Degree of

MASTER OF SCIENCE IN MECHANICAL ENGINEERING

THE UNIVERSITY OF TEXAS AT ARLINGTON

DECEMBER 2015

Acknowledgements

I would like to express my sincere gratitude towards my school, UT Arlington and moreover am grateful towards my team (Formula SAE) for training and inspiring me to carry out research work in this field. It is indeed a pleasure to acknowledge Dr. Robert Woods for just not mentoring me but also sharing his experience and studies within the same field. It wouldn't have been possible without his guidance, and the same has helped me take pride in my work, which not only pertains as a research guide, but is also implemented in the working life, SAE Electric-2015.

It is indeed an honor to thank my team members who assisted me with design ideas, machine training, and my experimental work. To all my family and friends that helped me manage stress, further not letting me give up at any point, to be positive and patience was a key to success. I am grateful to all the professors on my committee for their precious time and feedback.

I would again like to take this opportunity to thank Dr. Woods for his guidance, wisdom, positivity, inspiration, extensive experience and past work which plays a vital role in this thesis.

November 24, 2015

Abstract

HEAT REMOVAL ANALYSIS USING NTU/ MICROSCOPIC THEORY AND EXPERIMENTAL FLUID TESTING OF RADAITORS, PUMPS AND FANS FOR THE THERMAL MANAGEMENT SYSTEM OF FORMULA SAE ELECTRIC RACECAR

Shahzad S. Bulsara, MS

The University of Texas at Arlington, 2015

Supervising Professor: Robert L. Woods

Formula SAE at UT Arlington has always been building well engineered race cars, further being one of the top teams in The United States. However, an electric race car being first in the fleet, cooling of electric motors played a vital role. The thermal system being significantly different from combustion cars, consists of a lower heat application. It is always favourable to maintain electronics as close to ambient temperature as compared to its counter hydro-mechanical engines. To attain the objective, a complete thermal & fluid analysis was carried out using the NTU method/ microscopic theory and experimental results associated towards achieving system resistances/ pressure drop relations using frictional factors for the appropriate size of a dual pass radiator, water booster pumps and high profile fans.

Further, with system and pump/ fan curves, I received forecasted and actual operating points which in turn enables the team to have a better judgement and analytics towards the selection of the same.

Table of Contents

List of Illustrations

List of Tables

Chapter 1

INTRODUCTION

Radiator Package

It is defined as a sub system which is connected to a heat source (system of focus) in order to maintain the latter at its optimum temperature, further resulting in an overall balanced system performance.

In our case, the system of focus are the 4 in-wheel electric motors (Parker) which need to be cooled and further maintained below 70ºC especially for the MOSFETs, which act as electronics for the motors. The threshold point of motors to avoid depolarization is 85ºC. As far as electronics is concerned, the lesser the temperature, the better it is for them to work efficiently without problems. Unlike a combustion engine, the fluid (water in my case) circulating in this system is desired to flow at a lowest possible temperature, almost equivalent to room temperature. Furthermore, you also don't want to expend a lot of energy on this system to make it heavier, as well as pull in more amps which in turn works against us during endurance or as a matter of fact, the objective of car weight reduction.

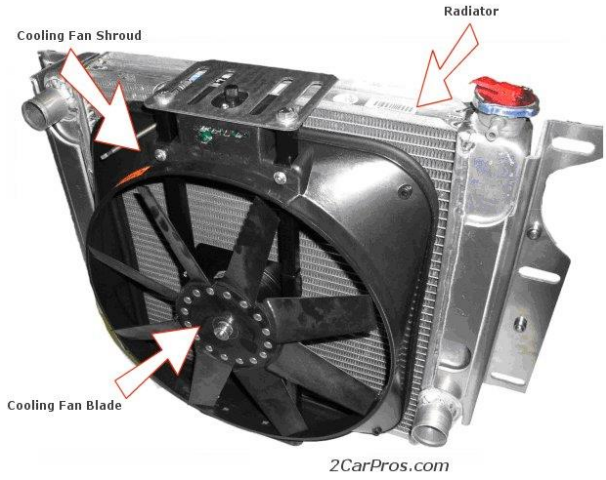

Figure 1-1 Radiator Package (reperesentation only)

System Layout

I had to decide upon 3 options for the piping layout which was complete series, complete parallel or a combination of both. The latter most gave an optimal solution which reduces weight, complexity of the lines running through the car as well as maintaining all the motors at almost same temperatures.

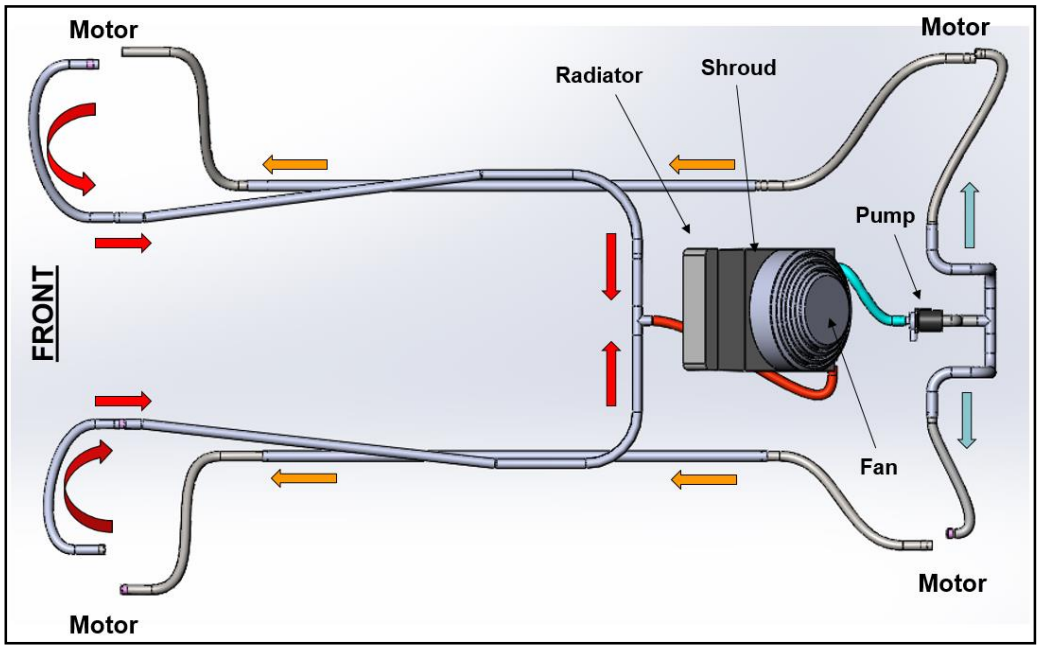

Figure 1-2 Piping Layout

Further, the rear motors produce twice as much power as the front, and hence water flows in the rear motors first in parallel and then obeys the series rule for entering on their respective sides, the front motors. The outlet of the front motors again use parallel combination, which is why it is termed as a combination of series and parallel. Demerits of only parallel combination include, 60% increase in pipe length, 6 tee joints and pipe layout complexities.

System Components

Radiator

The below radiator is designed on SolidWorks which represents a close to an accurate design as that of a Griffin radiator.

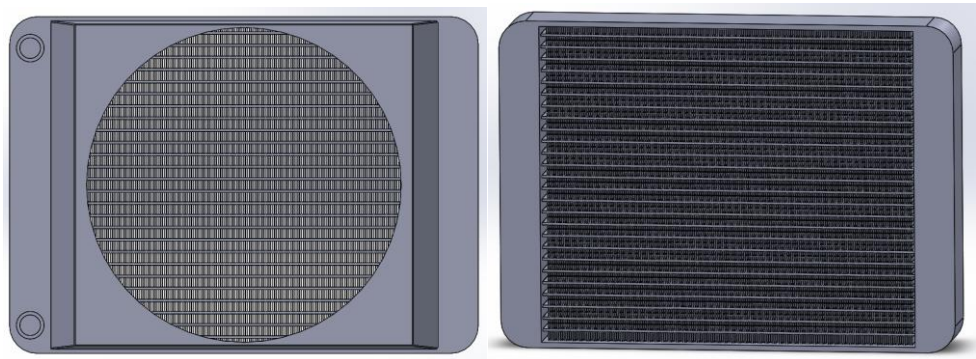

(a) (b)

Figure 1-3 Two sides of the designed radiator (a) with shroud and (b) opposite side

It is a dual pass cross flow type radiator consisting of 10 tubes in a single pass i.e. 20 tubes dual pass. The material used is Aluminum Alloy 3003 series for which the thermal properties are considered. The dimensions are standardized as mentioned in the pdf files on Griffin website. My analysis considers 220 fins per row (justified as 17 to 19 fins/inch). The reason for deciding upon 0.75 OD for the inlet/ outlet is that we have more standardized pipes and pump inlets for ¾ inch which results in a lesser pressure drop. Further, this complete package involves the arrangement of a fan with a shroud on the radiator core area.

Cooling Medium

The system uses pure water as mentioned in the FSAE 2015 rulebook which means a denial to the use of glycol. The steady state temperature for the system is

approximately 50ºC and further the thermal properties are considered for the same. We could have used oil as well but it would lead to a larger flow rate and bigger tubes. Further, the thermal conductivity of water is almost four times and the specific heat is twice as much compared to oil. Lastly, distilled water is low on initial as well as running cost.

Flexible lines/ hoses & clamps

Figure 1-4 Hoses & Clamps (representation only)

These flexible lines shall be used in complicated pathways such as the radiator to pump, pump to motor through zip tied formations on the A arms (suspension). The inlet diameter will be ¾ inch and further clamps placed on every connection. The application doesn't require high pressure as well as high temperatures. They need to be stiff but flexible, which in turn means a lower radius of curvature.

Hard lines

Figure 1-5 Aluminum lines (representation only)

The inflexible lines will be Aluminum 6061 as it maintains a good balance in weight and conductivity as compared to copper and steel. These pipes have to be equal in length

to maintain the system symmetry. Further, McMaster has good rates for the same. Furthermore, as planned the OD for these tubes shall be ¾ inch.

Tee's

Figure 1-5 Tee Joints (representation only)

As far as tee joints are concerned, we will require two of them on either sides of the car which will further split the mass flow rate almost equally when analyzed pragmatically. The ID of bends shall be ¾ inch, same as that of tee joints with the ID.

Water Pump

Figure 1-6 EBP 15 (represenation only)

For our analysis, we will need a pump throwing out 3.5 to 4 gpm. The selected pump should pull in less amps, have working pressure more than the pressure drop of the system, compact design, light in weight and driven by a 12V DC motor. The inlet/ outlet

dimensions connects a 3/4th inch hose adapter. Further the pump was finally bought from Davies Craig (Bosch pump). The pressure drop analysis will be discussed in the upcoming chapters.

Cooling Fan

Figure 1-7 Spal Fan (represenation only)

The fan was ordered from SPAL and from our calculations we will need 500 cfm as per our heat removal analysis. The same has been tested on the air flow bench available on campus (Woolf Hall #212). This is a 9 inch fan pulling (aspirante) 755 cfm at free flow condition and its tests shall be further discussed in the upcoming chapters in detail. The motor used is brushed DC (12 volts) and a high profile fan which suits my application.

Chapter 2

DETERMINING AVERAGE POWER

In order to come out with a number which determines the heat that needs to be rejected from the entire working system, we need to analyze the motor efficiency as well as the past track data which results in an average speed, further resulting in average horsepower. The efficiencies of rear and front motors are plotted from their relation with the rotational speed (rpm) and thus with the gearing ratio, energy that is lost as heat, is determined.

Track Data

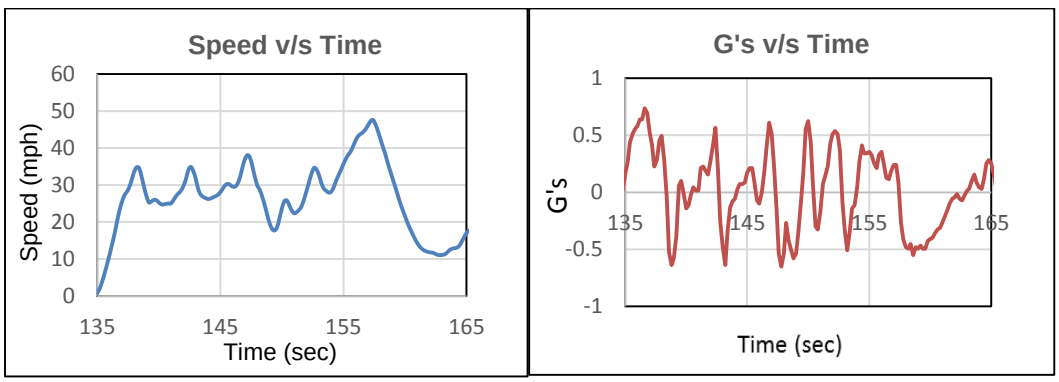

(a) (b)

Figure 2-1 (a) average track speed and (b) average track longitudinal G's

From the above graphs, it shows us the track data for the F-13 car (lap times and speed), speed and G's as a function of time. As a matter of fact the abscissa (time), a batch of data from 135 to 165 seconds was considered as it reflects one complete realistic lap which gives closer results for the actual performance at competition.

Further the average velocity of the car as observed is 33 mph and a value of 0.42 G's for the positive half of the cycles.

Motor Efficiencies

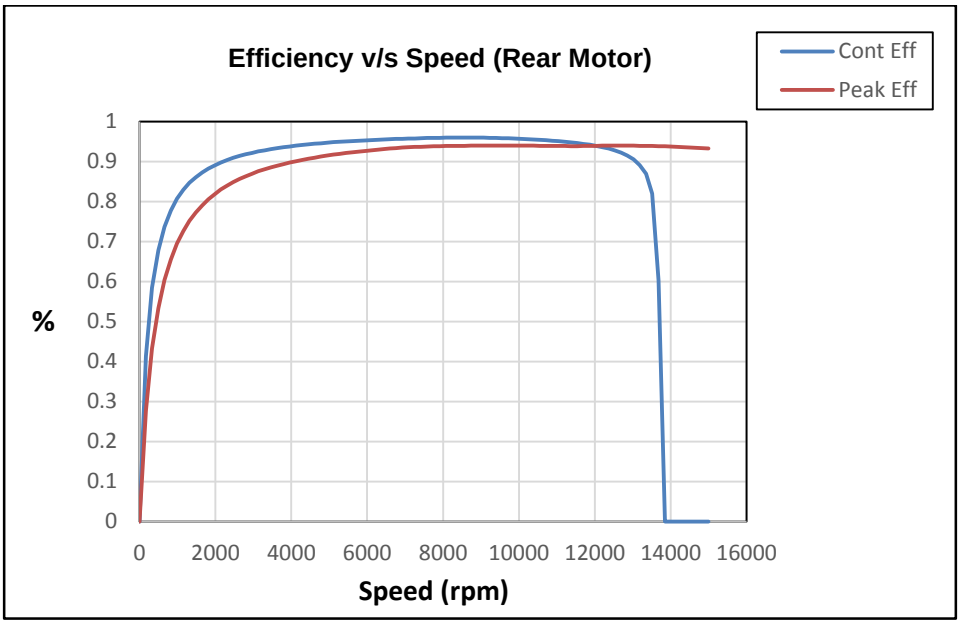

Figure 2-2 Rear Motor Efficiency

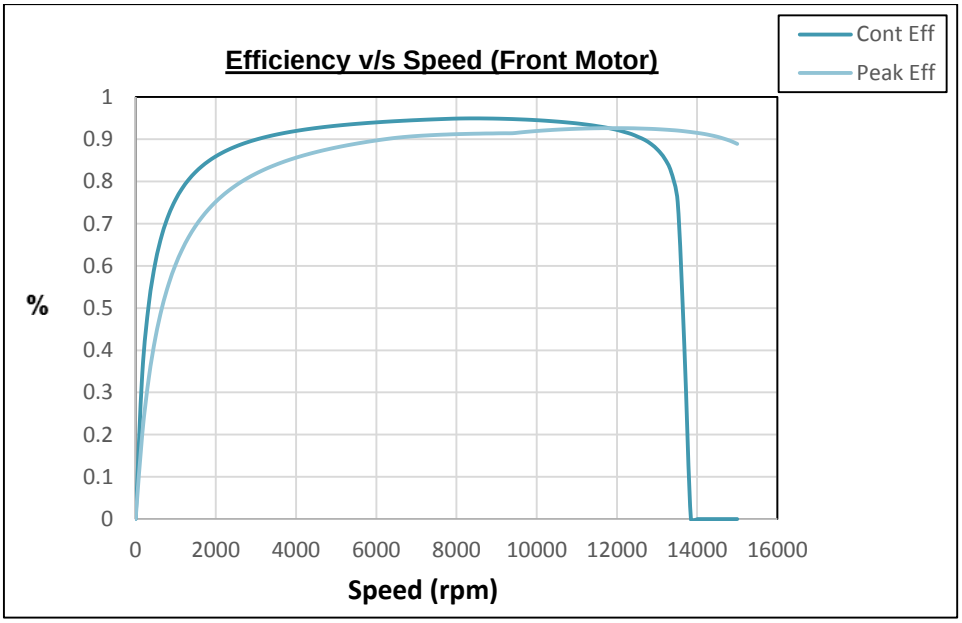

Figure 2-3 Front Motor Efficiency

From the above figures it can be seen that at several rpm we have attained different motor (rear & front) efficiencies. This efficiency less 100% gives us the remaining loss as heat which in turn is produced and needs to be rejected for an effective performance. The same has been illustrated in Appendix A Table A-1.

Furthermore, from the data that I received was analyzed in the form of a graphical representation for the rear and front motors as they possess different power capabilities. Each rear is 25 kW each, whereas the front are 12.5 kW which makes it half of the former one.

<u>Average Speed, Horsepower & Heat determination</u>

The Electric car Tire Diameter = 20.5 inches = 1.7 ft.

The ratio of gears used for motors and wheel = 12.83

The standard conversion of mph to rpm :-

mph = (1.7 * 3.14 * rpm * 60) / 5280

Thus, rpm = (33 * 5280) / (1.7 * 3.14 * 60) = 544 (wheel rpm)

Finally, Motor rpm = 544 * 12.83 = 6980 rpm

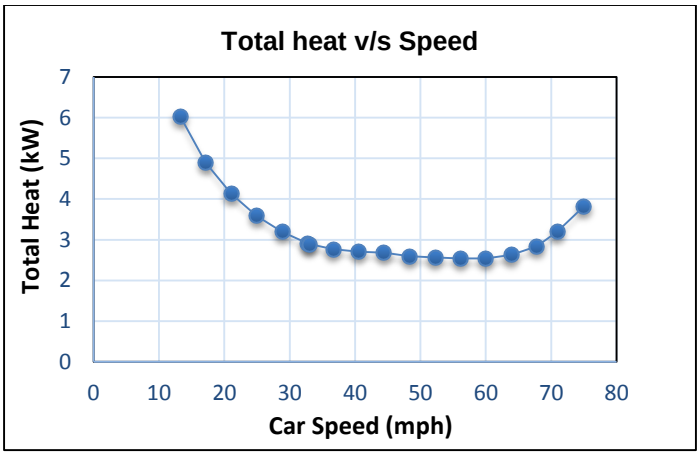

Figure 2-4 Heat produced at different speeds

Table 2-1 Heat produced at average speed

Motor Speed (rpm)	**Car Speed** (mph)	**Heat Produced** (Each Rear) %	**Total Rear Heat** (%)	**Heat Produced** (Each Front) %	**Total Front Heat** (%)	**Total Heat** (kW)	**Safety Factor** (SF)
6980	33	6.5	13.0	9.3	18.5	2.9	1.4

As calculated above the motor rpm is analyzed with the efficiency Table 2-1 and graph which finally results as an efficiency which further gives us heat produced. Similarly, heat at different speeds can be well predicted. The safety factor mentioned is the average considered for all speeds depicting values more than 1. For a complete reference of Table values, please refer Appendix A Table A-2.

Furthermore,

Average Horsepower = Mass Gravity G's Average Speed

= 320 (kg) 9.81 (m/s^2) 0.42 14.75 (m/s)

= **19.5 kW** = **26.2 HP**

For the average speed of 33 mph, we obtain motor efficiencies further which results in the amount of heat produced as a function of average power.

Average longitudinal G's are considered to be the rms value of all the G's in the track field. The negative signs too are considered as we have regeneration taking place within the electric motors which is not the case with combustion cars.

Rear Motor HP = 6.5% (heat) x 2 (motors) x 19.5 kW = **2.54 kW**

Front Motor HP = 9.25% x 2 x (19.5/2) (half power) = **1.8 kW**

Both of the above values are total heat numbers for front and rear respectively.

Table 2-2 Additional MOSFET heat

MOSFETs (kW)		Total Heat (kW)
Rear	0.1 x 2	0.2
Front	0.05 x 2	0.1
Total	0.3	**0.3**

Additionally the heat from the **MOSFETs** (Electronics) also has to be accounted for, which is going to be 0.1 kW each rear and 0.05 kW each front. Thus the total heat that the system has to be designed for is **4.4 kW**. It is the electronics that plays a vital role as far as maintaining the temperature at 70ºC is concerned.

Please note that the safety factor is considered only for values well above 1 to design the system with relative factor of safety.

Conclusively, I had to design my system for 4.4 kW which is definitely 1/5th of the heat that is rejected by its counter I.C. Engines. Hence, for such a low heat application, considerations in design as far as capacity of the system and their behavior within the installed environment differs significantly.

Chapter 3

HEAT REMOVAL BY NTU/ MICROSCOPIC THEORY

As far as heat rejection from a radiator is concerned, heat transfer through convection plays a vital role as compared to conduction and radiation. Convection is that mode of heat transfer that takes place through fluid i.e. water and air in my case of research and design. The concept of forced convection comes into picture when designing a cooling system which is carried out with electromechanical devices such as pumps and fans for water and air respectively.

Some of the laws followed are as follow:-

- Newton's law of Convection

$$Q = h\ A\ (T_s - T_\infty)$$

- First law of Thermodynamics

$$Q = \dot{m}\ C_p\ (\Delta T)$$

- Fourier's law of Conduction

$$Q = k\ A\ (\Delta T/L)$$

Where,

Q = heat rejected or absorbed (kW)

H = heat transfer coefficient considered for the fluid (kW/ m^2 ºC)

A = surface area or area perpendicular to heat travel (m^2)

T_s = surface temperature of the motor or radiator (ºC)

T_∞= fluid temperature (ºC)

K = thermal conductivity (kW/ m ºC)

ΔT = Temperature difference between inlet and outlet (ºC)

L = length of path of heat travel (m)

Math Model of the system

Further below stated is the math model for the system which shows the equations in relation to other components as far as thermodynamics is concerned.

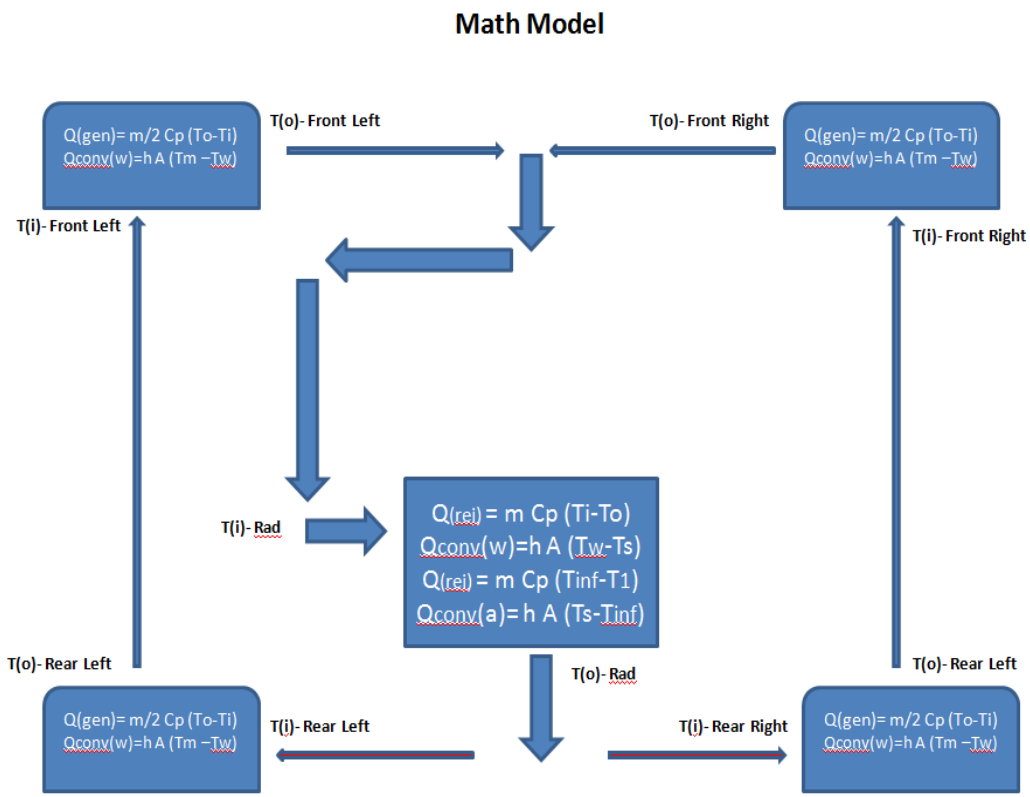

Figure 3-1 Equations around the system

NOTE:

T(o) - Radiator = T(in) - Rear Right = T(in) - Rear Left

T(o) – Rear Left = T(in) Front Left = T(o) Rear Right = T(in) Front Right

T(o) – Front Left = T(o) Front Right = T(in) Radiator

Heat rejection through radiator

Radiator analogy

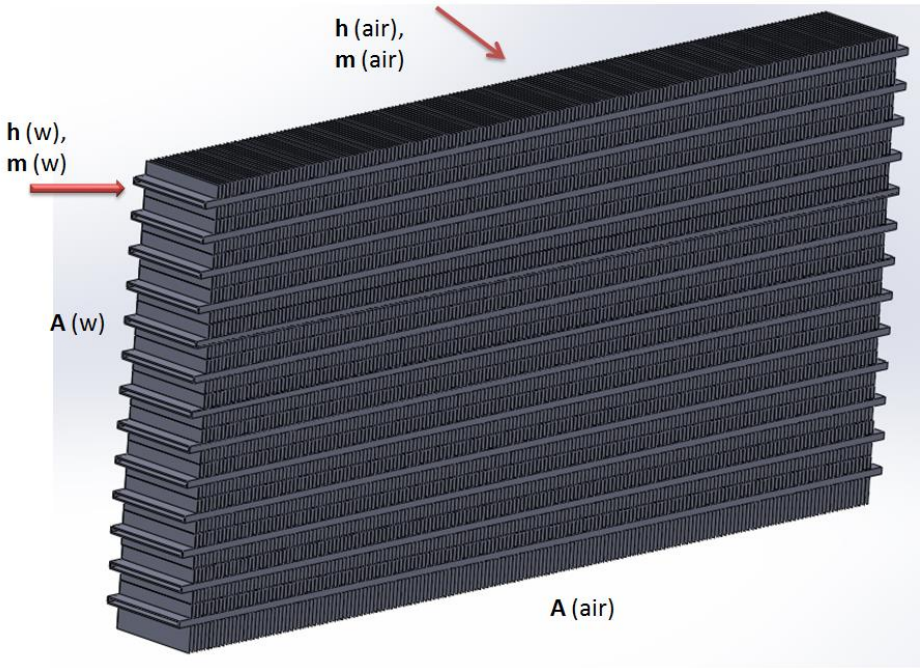

Figure 3-2 Heat rejection through radiator

A dual pass radiator was considered as it does involve a greater temperature drop as compared to a single pass. The problem with the triple pass lies with the trade off between pressure drop as compared to heat removal. Fluid dynamics will be dealt with in the succeeding chapters. I have considered the tubes to be rectangular which is almost similar to the actual cross-section of the radiator tubes.

As shown in Figure 3-2, fins on a radiator definitely increase the surface area which is better for the heat transfer to take place but comes with a trade-off with the resistance to heat travel and that's where we have to consider fin efficiency. However, the conductive heat transfer through the system is negligible as compared to the convection taking place.

Radiator configurations

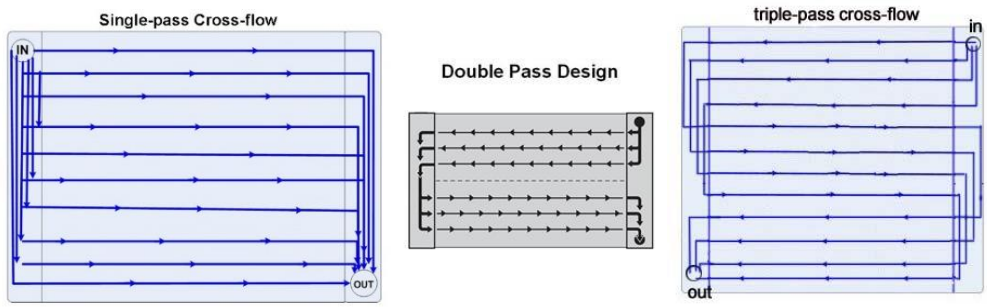

(a) (b) (c)

Figure 3-3 (a) single pass (b) dual and (c) triple pass

The types of radiators that were well analyzed were single, dual and triple pass with cross flow configurations. Even though we receive a greater temperature drop which is because of more flow length and velocity, but not at the cost of a greater pressure drop which restricts and demands for more power. For example, with a triple pass radiator, you would get a greater temperature drop but the pressure drop increases exponentially which is not desirable. Also, we didn't have triple pass radiators to test for their pressure drop. A dual pass is the one which is most prominent in many applications as it possess a correct balance in between heat transfer as well as pressure drop.

Convective heat transfer coefficient

Determining the convective heat transfer coefficient, is the major part of the study that was carried out in this research. The calculation or estimation of these coefficients is solved through dimensionless numbers such as Nusselt, Reynolds and Prandtl. In this section, we shall discuss the behavior of a fluid flowing with an objective to reject or absorb heat.

Nusselt's relation is the most important of all and it varies with the application, i.e. the way fluid flows through a tube, horizontally or circumferentially.

$$Nu = \frac{h\,D}{k} \qquad Re = \frac{D\,V\rho}{\mu}$$

$$Pr = \frac{\nu}{\alpha} = \frac{\mu\,C_p}{k}$$

Dimensionless Numbers used in Forced Convection Heat Transfer Coefficient Correlations

D = characteristic length (diam. for pipe), ft or m
V = characteristic fluid velocity, ft/sec or m/s
k = thermal conductivity of the fluid, Btu/hr-ft-^{o}F or kJ/hr-m-K
ρ = density of the fluid, slugs/ft^3 or kg/m^3
μ = viscosity of the fluid, lb-sec/ft^2 or N-s/m^2
h = heat transfer coefficient, Btu/hr-ft^2-^{o}F or kJ/hr-m^2-K

Figure 3-4 Dimensionless numbers used for coefficients (representation only)

The convective coefficients are obtained from the specific Nusselt number that is used according to the application that the flow of the fluid is meant to be behaving.

Table B-1 and B-2 in Appendix B shows the table of values for convective coefficients for air at 500 cfm and water at 4 gpm respectively. The application of air and water uses different relations of Nusselt number as water flows horizontally in tubes and the air flows through fins. Further, it is due to the hydraulic diameter that the velocity can be determined which in turn justifies the flow to be either laminar, transitional or turbulent. Turbulent applications justify greatest possible heat transfer. The concept of hydrodynamic and thermal boundary layers will be further discussed.

Hydrodynamic and Thermal boundary layers

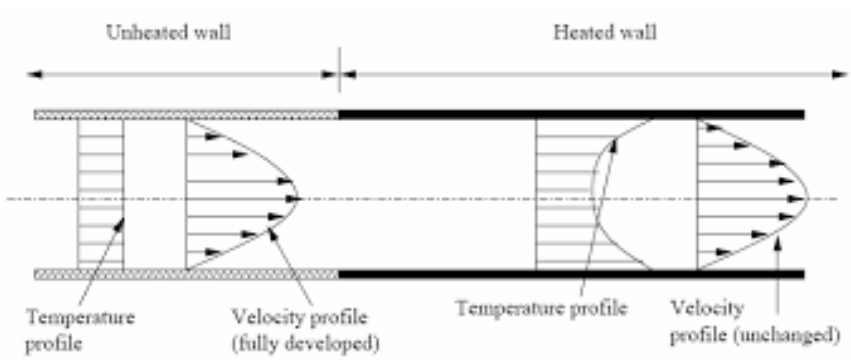

Figure 3-5 Flow though a pipe (representation only)

As shown in Figure 3-5, one has to consider for the flow to be hydrodynamically and thermally developed or developing. Thermal boundary layer plays a more vital role as heat transfer is the main objective of the system. We can control hydrodynamics as it depends on the velocity of the flow through a pipe.

The critical Reynolds number for a flow in a rectangular pipe is 3000 and any number below 2300 makes it laminar. The above boundary layers play a significant role when the flow is laminar, otherwise, as the velocity increases so does the turbulence which helps us neglect these lengths.

In short, complications start arising as and when the flow is laminar.

We have different types of flows:

- Fully developed
- Hydrodynamically developing & thermally developed
- Thermaly developing and hydrodynamically developed
- Simultaneously developing

The hydrodynamic entry length for laminar flow is given by,

- L_e / D (apprx.) = 0.05 Re

Thermal entry length for laminar flow,

- L_e / D (apprx.) = 0.05 Re Pr

Thermal & Hydrodynamic lengths for turbulent flow,

- L_e / D = 10

Thermal boundary lengths are always greater than hydrodynamic lengths for fluids with Prandtl number greater than 1 which is in most of the cases.

In the heat transfer calcualtions, I have considered these boundary layers only for Reynolds below 2300. For others, a relation for fully developed flow has been considered for calculative purposes.

Further, we shall discuss the different relations used for Nusselt number depending on laminar or transition, as well as according to the flow pattern. My research consists of the following categories of flow

- Simultaneously developing flow (Nusselt's Eqn. for constant heat flux)

(3-1)

The value of 4.364 is valid for circular pipes, but in our case of rectangular tubes and the derived aspect ratio, it will be 7.7 which pertains to a value of fully developed.

The above Equation 3-1 is valid for 0.7<Pr<7, Re< 2300, Re.Pr.D/L < 33, with D as the hydraulic diameter and L as the length of the pipe designed or considered.

- Fully developed flow (Nusselts equation for constant heat flux)

(3-2)

Where the friction factor for Equation 3-2 is given by,

Equation 3-3 is valid for Re > 2300 which is for turbulent as well as transitional flows. It is the application of this equation which doesn't consider thermal and hydrodynamic boundary layers in my analysis as it can be neglected.

The heat transfer analysis for the water flow rate considers simply Equation 3-1 for laminar flow which is derived for simulataneous developing and Re lesser than 2300, for the rest we won't be considering the lengths as the period of transition is difficult to forecast a perfect equation, hence fully developed can be used for Re greater than 2300.

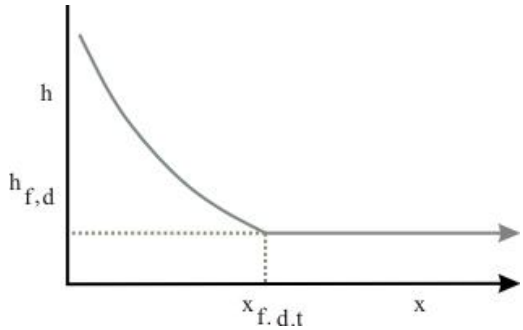

Figure 3-6 Variation of heat transfer coefficient with length (representation only)

The convective heat transfer coefficient reduces and then comes to a constant value with the flow being fully developed as shown in the Figure 3-6.

In the case of thermal boundary layer, unless the flow is developed there won't be maximum temperature difference in between the surface and fluid, but the heat transfer is as per desired because the value of 'h' is higher than the desired temperature difference.

As and when the flow is fully developed we can be accurate in assuming a constant value of heat transfer coefficient, which is in turn due to Nusselts number.

Study of NTU & LMTD method

A detailed study was carried out regarding the consideration of the above two methods. The log mean temperature difference is more of an experimental approach as it requires the inlet and outlet temperatures of both the fluids which is not possible without an experiment. Secondly, the number of transfer units enables us to get ready with a complete analytical process of rejecting heat by assuming the atmospheric temperature and the hot side of the coolant.

Before getting results of effectiveness and maximum possible heat transfer, the heat transfer coefficients for different flow rates of water and air are shown in the below graph.

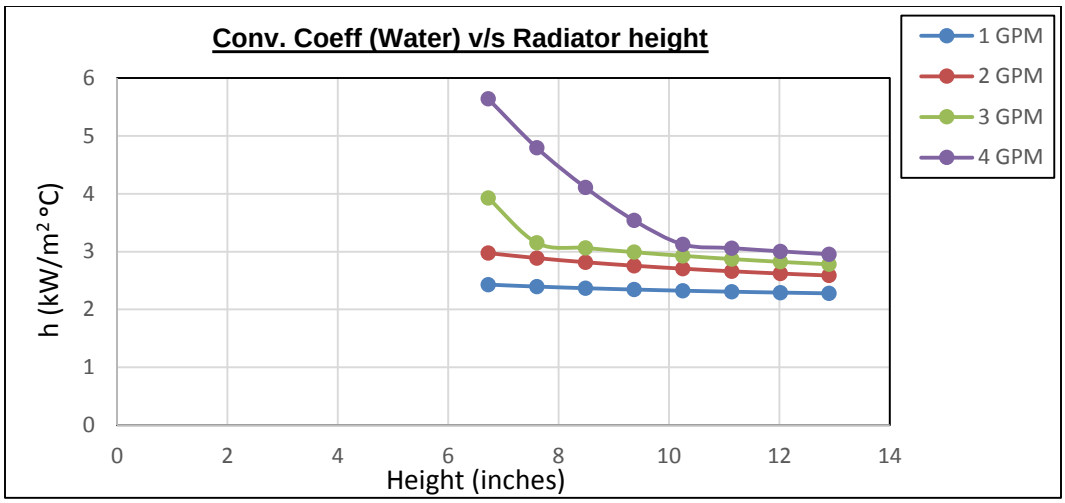

Figure 3-7 Dual pass radiator with different number of tubes

The water properties at a working pressure of 3 psi and 50ºC are considered for calculations. As the temperature of fluid increases, so does its flow velocity which further increases heat coefficients.

In the Figure 3-7, we can observe that for higher flowrates the graph does resemble figure 3-6, which is due to the Nusselt's equation considered and explained above.

Similarly, for calculating the heat transfer coefficients for air we use the following co-relation for Nusselt,

$$Nu\ (air) = 0.664\ \ Re^{0.5}\ \ Pr^{0.33} \qquad (3\text{-}4)$$

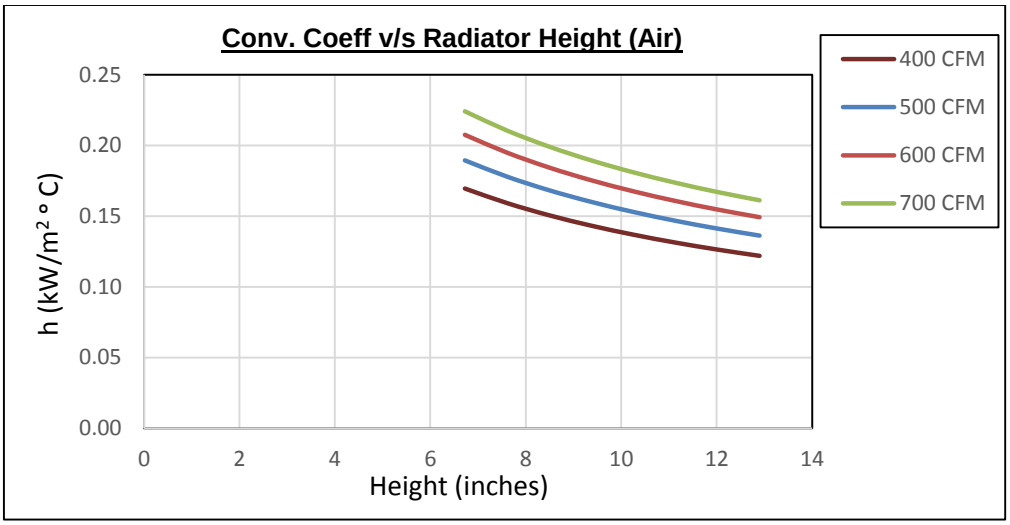

Figure 3-8 Radiator for different tube numbers

Figure 3-8 illustrates the heat transfer coefficients for air that flows through the radiator core. Irrespective of the radiator being a single or dual pass, the above graph won't change as the external structure remains the same.

Atmospheric air at 30 degree celcius are considered for analysis on the air.

Note that the hydraulic diameter of air is calculated as follows, the credit of which purely goes to Dr. Woods,

$$d_h = \frac{4A}{P} = \frac{4\left(\frac{\frac{2}{FD}Wf}{2}\right)}{\left(\frac{2}{FD} + 2\sqrt{\left(\frac{1}{FD}\right)^2 + W_f^2}\right)} \tag{3-5}$$

where,

FD = fin density

W_f = width of each row in between tubes

Further the calculated heat rejected with different iterations for air, water flow rate and sizes of the radiator that can be suited for my application which has space restrictions.

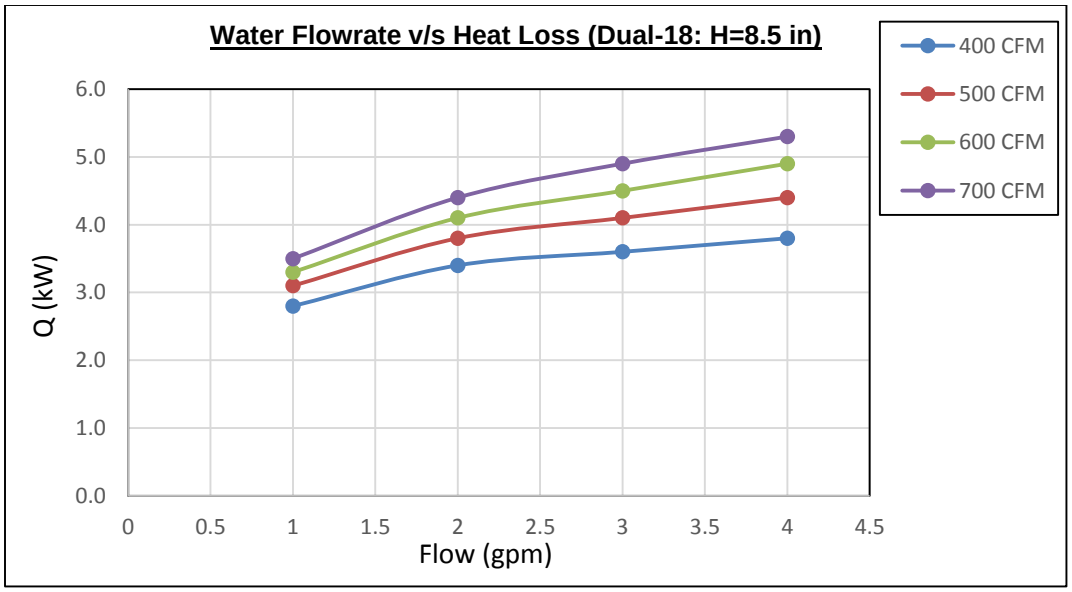

Figure 3-9 Heat removal at different fluid flow rates

Figure 3-9 illustrates the heat removal from a dual pass radiator with 18 tubes which makes a height of 8.5 inches. The length of the radiator core is always kept constant on the basis of space restrictions. Hence, the maximum possible length that could be possible is 12.4 inches. The tube sizes along with the fin density is considered the same as that of information provided by Griffin (company that manufactured this radiator).

Finally the radiator that accomplished an appropriate result consists of 20 tubes and thus the core size for this design is 12.4 in. x 9.4 in. The heat transfer taking place in Figure 3-10 is greater than a single pass but lesser than a triple pass for the same size and flow rate of fluids.

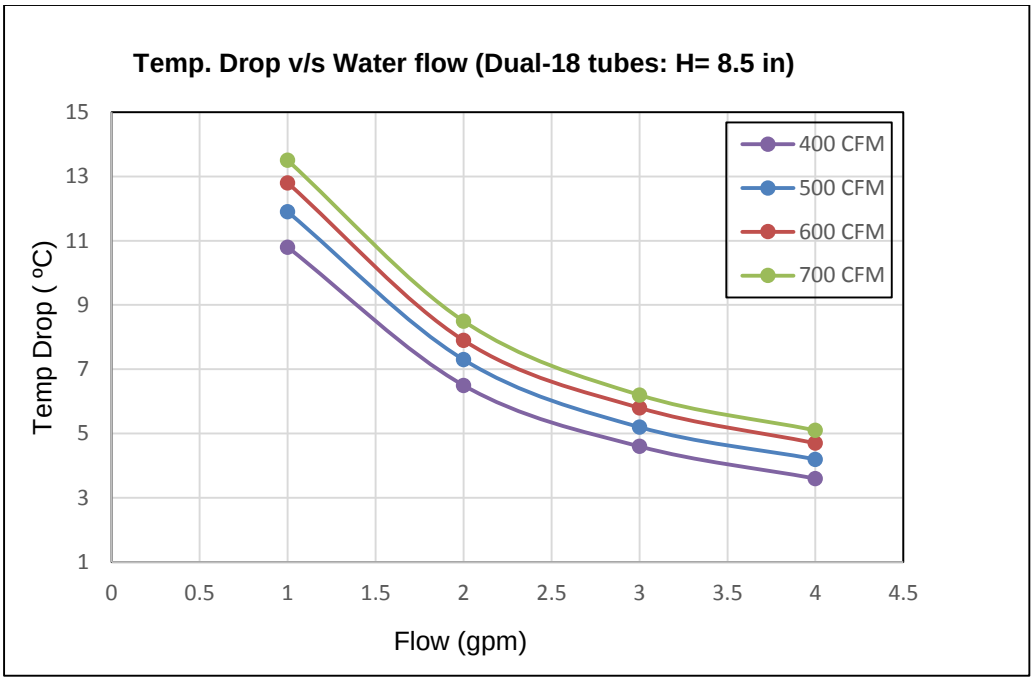

Figure 3-10 Temperature drop at different fluid flow rates

Figure 3-10 shows the temperature drop with the same radiator that heat was analyzed for as in Figure 3-9. We can observe with 1 gpm of water flow rate, we have greater temperature drop but not the heat removed as per our earlier calculations (4.4kW).

In order to remove more heat, we have certain controlled factors which can be taken into account. For a greater temperature drop and same heat removal, use a higher CFM as well as a greater size of radiator. The same can as well be attained with a higher water flow rate but we wouldn't receive greater temperature drop. In the case of electric motors, the lower the temperature, more efficient can the electronics be for the car's endurance track. The same above i.e. temperature drop, heat removal and convective coefficients are displayed calculatively in Appendix B.

Microscopic theory of heat removal

This is completely my theory which is used to ensure or in short re-check the above NTU method. This theory doesn't reflect numbers with relation to effectiveness, hence gives values of heat rejection much above of what actually is rejected or aspired. It is quite of a methodical process which calculates heat rejection through a step by step process.

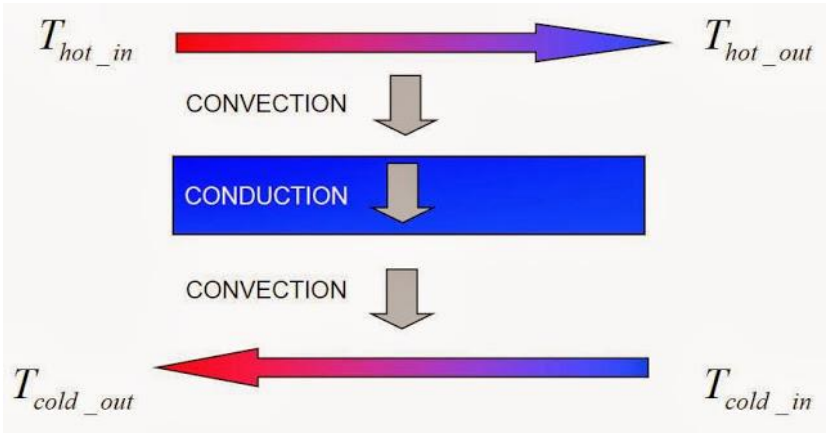

Figure 3-11 Step wise heat rejection (representation only)

- Heat rejected by the water while travelling through the tube.
- The same heat travels through the law of conduction towards its length and thus we get average of the values throughout its length as the temperature differs which is defined as efficiency of a fin.
- Further, the required convective coefficient is calculated to the average surface temperature of the tubes and fins.
- Lastly, the actual convective coefficient is calculated through dimensionless numbers as discussed in the previous sections of the chapter.

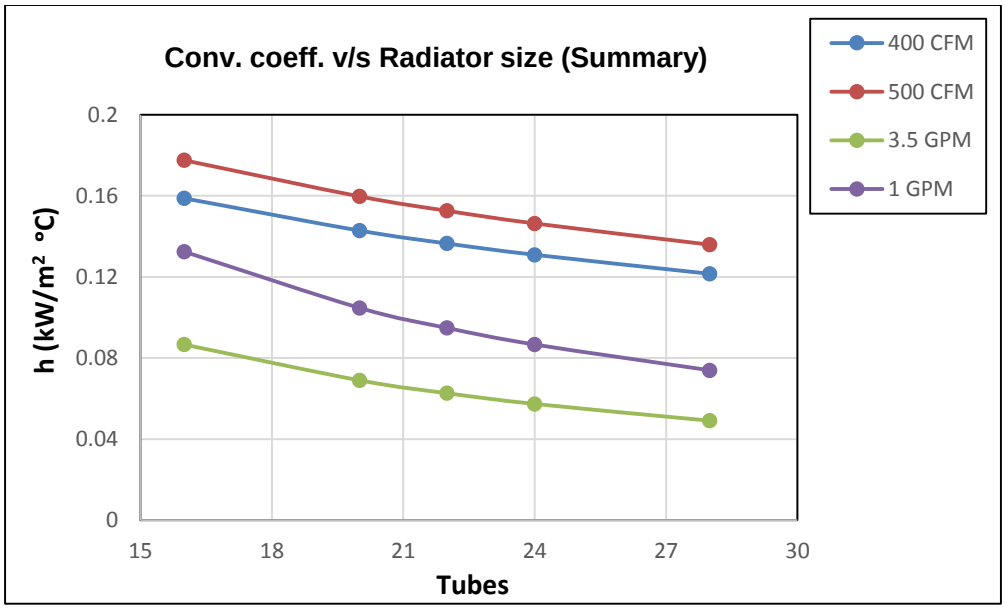

Figure 3-12 Comparison of actual & required heat coefficients (air)

The lines for 1 and 3.5 gpm are iterations for the required heat transfer coefficients for air, and the ones for 400 and 500 cfm are the coefficients actually possible with those fans.

Here we can see that the actual coefficients received for the same number of tubes is much more as compared to the desired. This is because the effectiveness of the system (radiator) is not considered.

To remove a specific amount of heat, one's average water temperature has to be certain degrees higher as compared to the ambient temperature.

In the case of a heat engine, it runs much higher as compared to electric motors and the latter is desired to run as close to the ambient as possible. This is possible only and only when the water is higher than the air temperature in order to remove the desired heat out of the system.

NOTE: The entire system is designed at steady state (one cycle)

Heat rejection through motors

Electric motor analogy

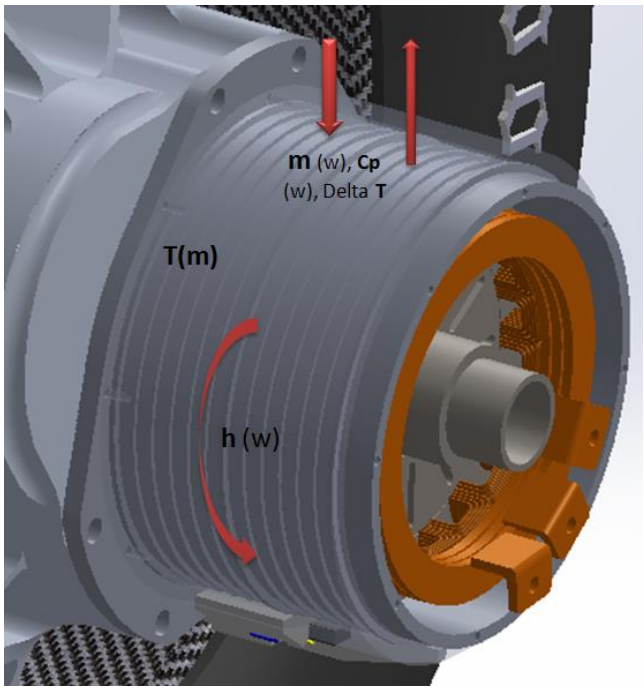

Figure 3-13 Heat transfer through motors

After analyzing the radiator, comes the heat source which doesn't necessitate the use of NTU for heat rejection. The equations used are similar to that of the one illustrated in the beginning of this chapter.

Even though air flows above the motors, heat transferred to the air is not accounted for which is an additional safety factor for the system design.

In further sections we shall discuss forced convective coefficients and heat transfer through the motors which is almost similar to the case of the radiator.

The water properties are again considered at 3 psi and 50ºC which is the steady state temperature of the system.

The Nusselt's relation used for motors is similar to that of fluid flowing across a cylinder. This gives an approximate result value if not accurate.

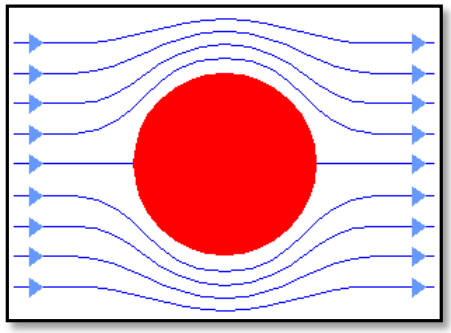

Figure 3-14 Water flow over cylinder (representation only)

Nusselt's equation for water is given below,

$$Nu = c\ Re^{m}\ Pr^{0.33} \tag{3-6}$$

Where,

c & m = constants 0.913 and 0.618 respectively for Reynolds number 4000 to 40000

Nu, Re, Pr = Nusselt, Reynolds and Prandtl as dimensionless numbers.

Further, the heat transfer coefficients of water flowing through the channels in the motor are discussed. As the cross sectional area of the channels in the motors are smaller as compared to the pipe diameter, we face a greater pressure drop due to the sudden increase in velocity.

The higher coefficient values show that the water with forced convection lies within the limits of 50000 (W/ m^2 ºC) for boiling water. This indeed depends on the value of Prandtl number which in turn depends on water properties.

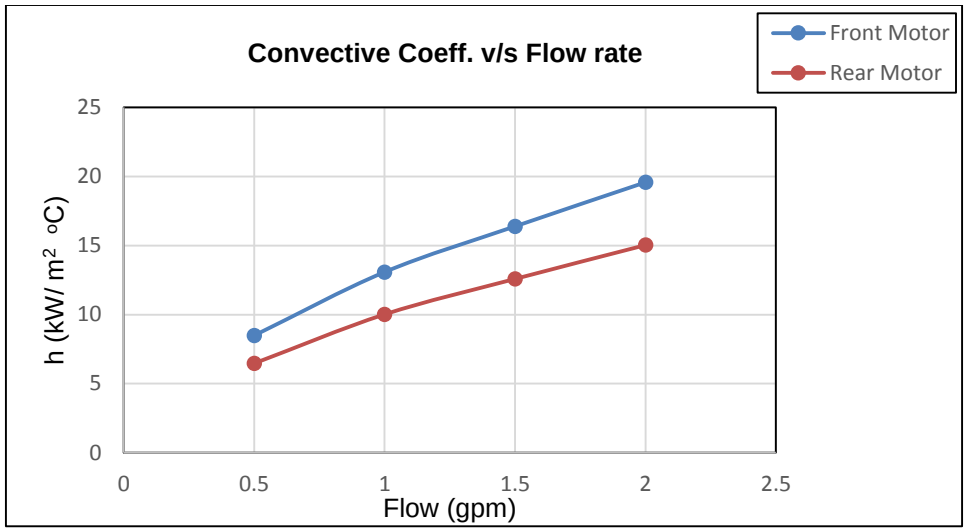

Figure 3-15 Convective coefficients of water for motors

The flowrate of water is reduced by half since it flows through a tee and hence splits into 2 (discussed in earlier chapters). The rear motor being bigger in size (only width) produces twice the power as compared to the front motors. However, the front is calibrated for 100% regen, while the rear one calls for 50% regen.

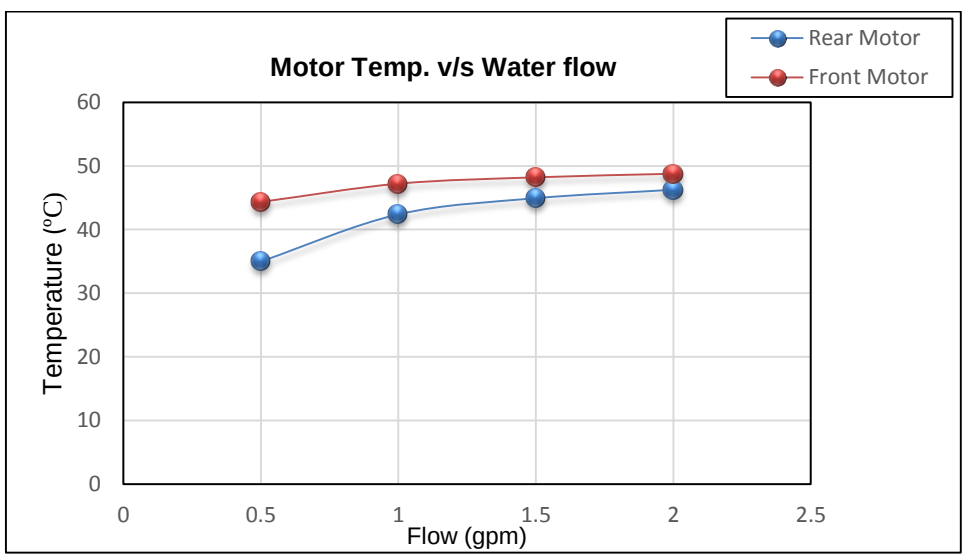

Figure 3-16 Motor temperatures after cooling

Simulation through MATLAB/ Simulink

The entire system is simulated which depicts similar results to the ones received in the previous sections of this chapter.

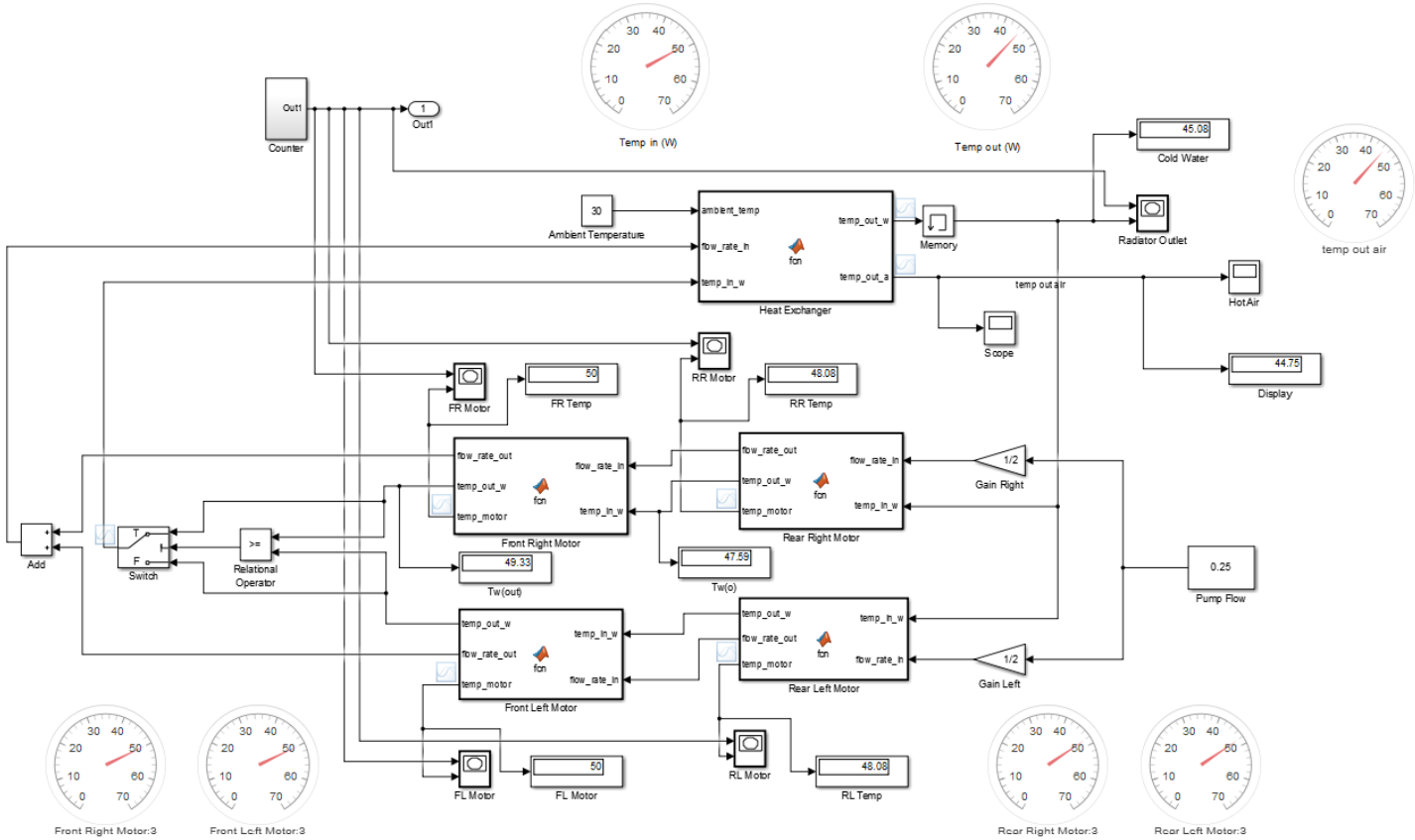

Figure 3-17 Simulink simulation of the complete system

MATLAB function blocks were simply used for the radiator and motors. The values obtained for the final pump and fan selected like convective coefficients, heat numbers, inlet temperature to the radiator was used as fixed values in the same. Figure 3-18 and 3-19 are snapshots after simulation runs for 50 seconds and is designed for steady state as stated previously.

Further results as far as graphs were concerned have also been shared as below.

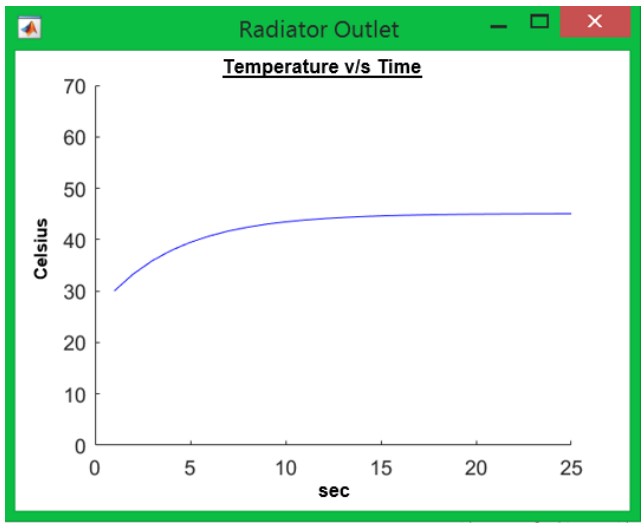

Figure 3-18 Hot water inlet to Radiator

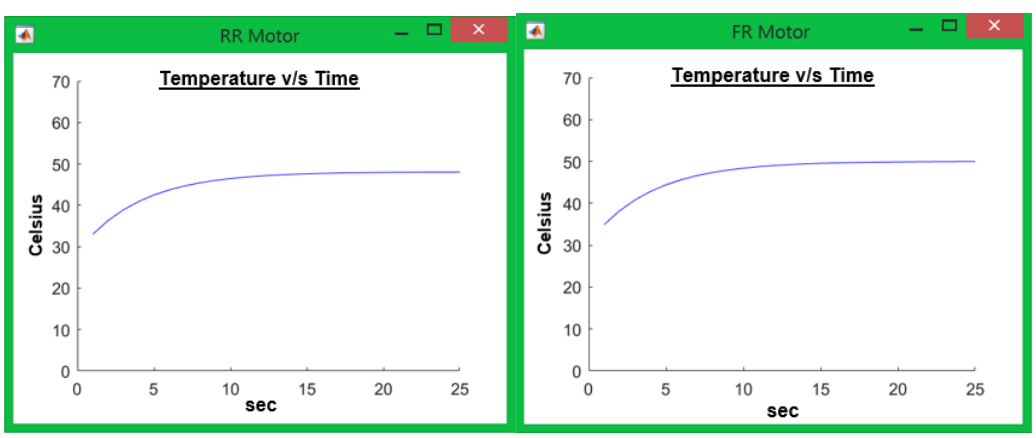

Figure 3-19 Temperatures of front and rear motors

Chapter 4

SYSTEM PRESSURE DROP

Fluid mechanics is that branch of physics which deals with the mechanics of fluids (liquids/ gases) and forces acting on them. It is divided in two sections, fluid statics and dynamics. The main focus in this chapter deals with hydrodynamics, even though aerodynamics is a part of fluid dynamics. Hydrodynamics is defined as that branch of fluid dynamics which deals with the motion of fluids, forces acting on them, lets say a case of a solid body immersed in a liquid bath.

This chapter deals with theories developed through equations and validating them through experiments as far as test on air and water is concerened. Many radiators were tested as system resistances and so were the pumps and fans as devices producing a forced convection to the system. The syudy of this chapters enlightens one to have a sharp judgement on the basis of pressure drop of devices and sub systems and their selection.

Friction factory theory using below equations

Resistance factor,

$$RF = \frac{\overline{N}}{A}\sqrt{f\,\frac{L}{d_h}} \qquad \text{(4-1) a}$$

Woods' number for water & air,

$$\overline{N} = \sqrt{\rho_{std}\,P_{std}} = 0.1426\frac{\text{lbf}}{\text{gpm}} \qquad \text{(4-1) b}$$

$$\overline{N} = \sqrt{\rho_{std}\,P_{std}} = 0.03666\frac{\text{lbf}}{\text{scfm}} \qquad \text{(4-1) c}$$

$\overline{N}$ is called Woods' number as this theory's recognition goes to him as it was formulated by him. The previously forecasted RF value is used in the first equation to get the friction

value (f). This theory is applicable for both water and air side of fluid analysis. The $\overline{N}$ is different for water and air as shown respectively. The average value can be used to determine RF value for our design and further predict water and air pressure drops.

Water pressure drop

In this section, five radiators were tested and a theory was developed along with an equation which passes through all experimental points. Further the resistance factor that is used to predict the curve later gives us results in the form of friction factor which then is used as a common term to predict the future designed radiator.

The process starts with the below mentioned equation that developes a curve which passes through all the practical results.

The system resistance for fluid flow is given below,

$$Q_{stc} = \frac{\sqrt{\left(\delta P_u + P_{atm}\right)^2 - P_{atm}{}^2}}{RF}$$

Equation 4-2 was used as theory to form the above exponential curves and it did work well for air and water pressure drop. Further this would lead to a final value of friction factor to predict pressure drop without testing radiators in the future. The RF value predicted in the above radiators is formulated from this equation. Further investigation can be done if any other equation could be applicable as I did with one of them (squares law), the coefficient of discharge method (C_d) which didn't fit well as the predicted values of discharge were way above the researched values of 0.6 to 1.

Tested Radiators

- Griffin Radiator

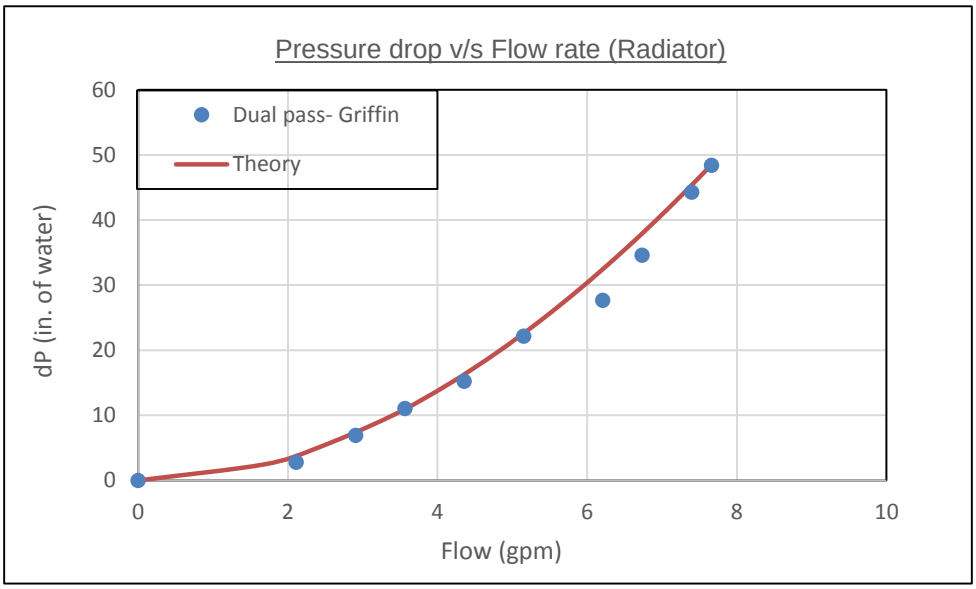

Figure 4-1 Griffin dual pass tested with developed theory

This is dual pass radiator with a total of 31 tubes and an inlet/outlet of 0.6 inches. A dual pass is supposed to have a greater pressure drop as compared to a single pass (almost twice). The blue dots on the graph depict the experimental values whereas the curve that fits in is the theory that is formulated. The forecasted value for resistance factor (RF) was found to be 26.7 inches of H_2O/ gpm.

NOTE: The apparatus setup is similar for all the tested radiators which includes a wall water supply connected to a flowmeter which is further connected to the radiator through a pressure gauge. Even though it is tested as an open system, one can avoid head losses by placing the radiator on a flat stiff plane as well as avoid the air trapped in the system initially.

- F-09 Racecar radiator

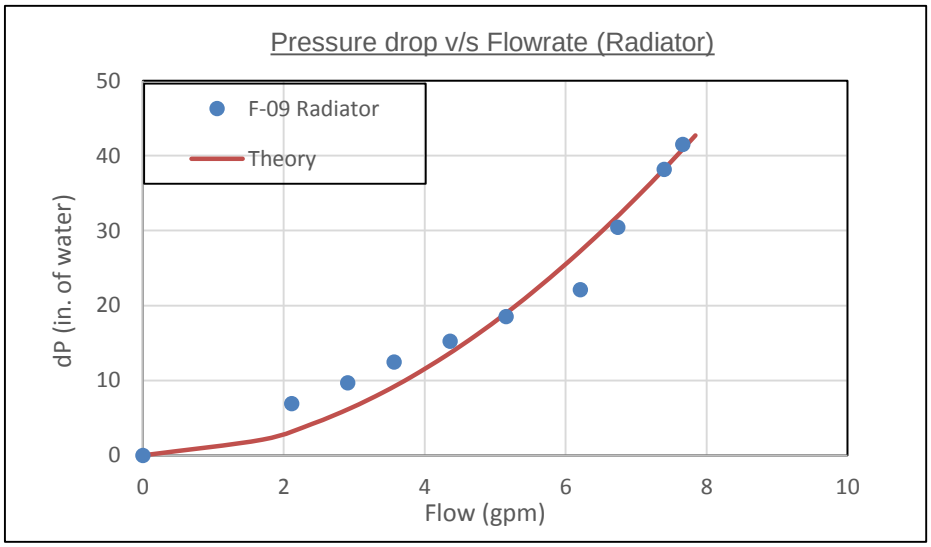

Figure 4-2 Formula 2009 dual pass tested with theory

The above radiator was removed from an existing running 2009 racecar and is a dual pass with a total of 48 tubes (double row), inlet/ outlet of 0.87inches. The radiator was tested similarly and its theory showed a resistance factor (RF) of 24.4 inches of water/gpm.

- Radiator by Long

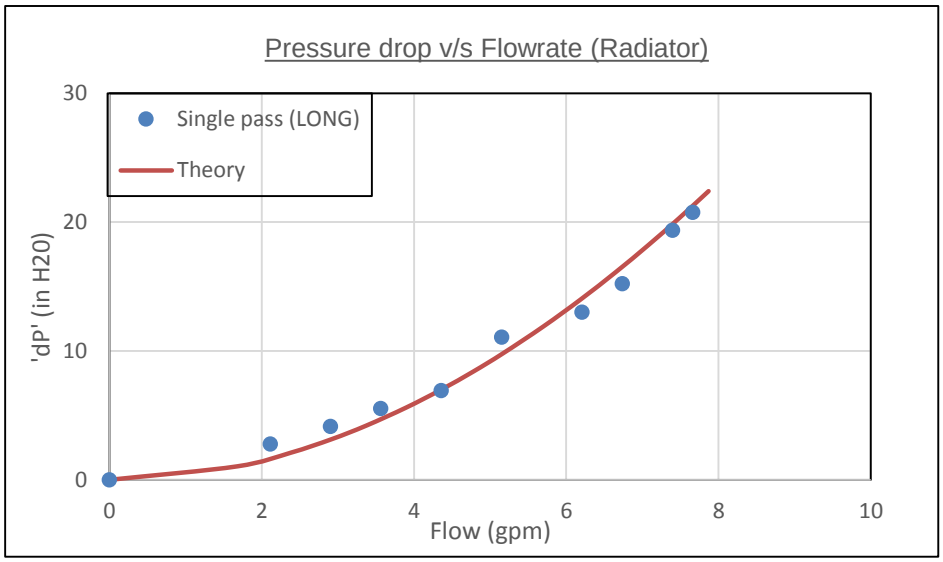

Figure 4-3 LONG single pass tested with theory

This radiator was given to me by Dr. Woods for acquiring more data as it is always great to have more data. This is a single pass (double row) manufactured by a company called LONG. Inlet/ outlet of 0.62 inches and resulted with an RF value of 17.4 inches of water/gpm. The theory resulted more accurately for this type and is close to the ones mentioned above.

- Local radiator

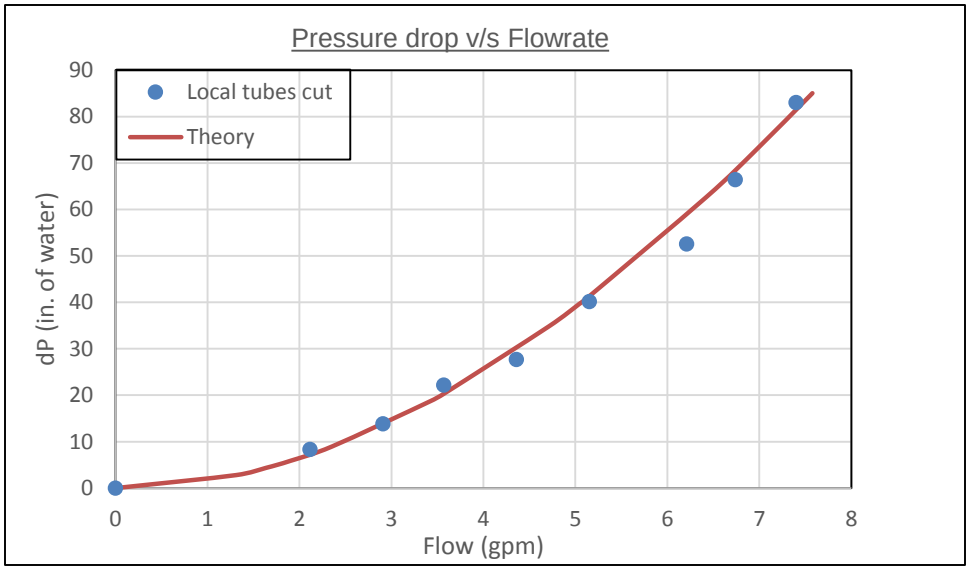

Figure 4-4 Local radiator tested with tubes

This radiator behaved really differently as compared to the others and hence wasn't considered while forming the final theory for friction factor. This is a single pass radiator with 38 tubes and inlet/outlet of 0.5 inches. The resultant RF value for this radiator was 36.5 inches of water/gpm which is way off from the others (maybe because of sudden reduction in the inlet/outlet area).

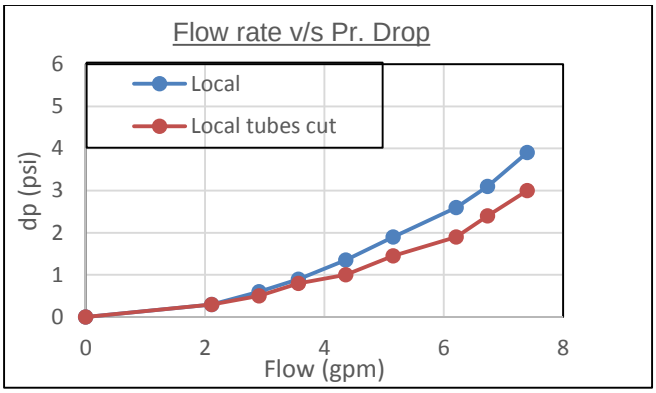

Figure 4-5 Local radiator after tubes cut

This radiator was further investigated. The below graph shows us the difference in pressure drop before and after the tubes are cut for testing. This radiator is not considered for its off results which physically is different from the rest tested.

- Wide radiator (Long)

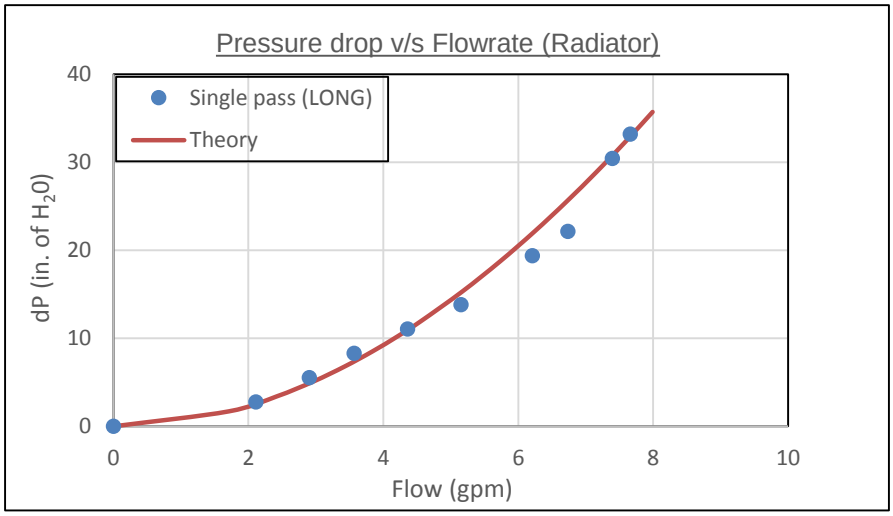

Figure 4-6 Single pass wide radiator by Long

This radiator did behave similarly as compared to its former ones. It is a single pass radiator manufactured by LONG with an inlet/ outlet of 0.62 inches, 26 tubes (double row), and a resultant RF of 21.8 inches of water/ gpm.

- E-15 Griffin radiator

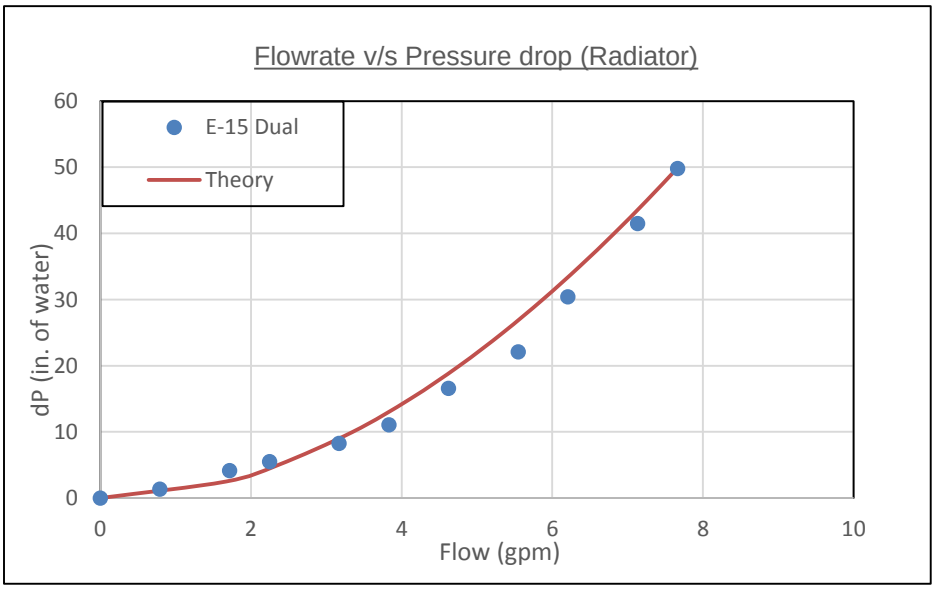

Figure 4-7 Electric car 2015 Griffin radiator

The current radiator was is similarly tested and I obtained results similar to common friction factors calculated from the resistance factors predicted as earlier.

Pumps

Figure 4-8 Pumps from Davies craig (Bosch) and Johnson

I considered 3 pumps for the application towards heat rejection from an electric car. 2 pumps were from Johnson (JP) and the third one will be from Davies Craig which is an Australian company. The free flow for the Bosch pump is 5.8 GPM and further the test for flow and pressure shall be illustrated.

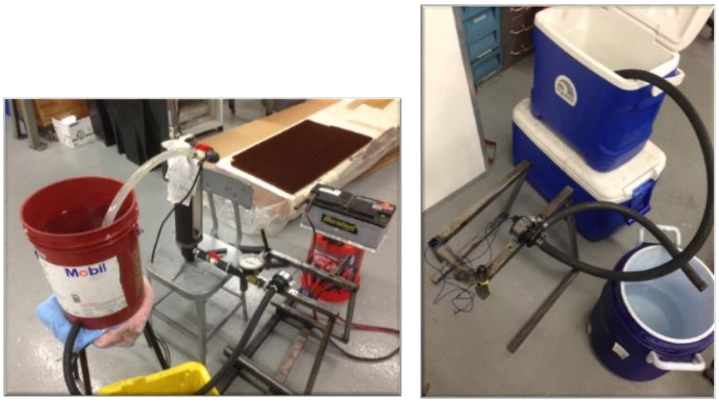

(a) (b)

Figure 4-9 (a) Pressure test (b) flow test on EBP-15

The flow results were almost the same as mentioned by the seller 1.9 gallons in 20 seconds which sums upto 5.7 GPM. The pressure test uses a flowmeter, a pressure gauge and was tested as a closed system which is further discussed.

Water flow summary

Table 4-1 Results to predict the future design with the actual radiator

Radiator	Pass	Inlet/outlet (in.)	Tube Width (in.)	Tube height (in.)	Hyd. Dia (in.)	L (in.)	RF (in. H2O/GPM)	RF psi/gpm	Entry tubes	Area (sq. in)	f
Griffin	Dual	0.6	1.21	0.05	0.096	14.25	26.7	1.0	15	0.9	0.25
F-09 by LONG	Dual	0.87	0.56	0.05	0.092	13.5	24.4	0.9	24	0.7	0.12
LONG	Single	0.62	0.56	0.05	0.092	9.8	17.4	0.6	48	1.3	0.33
Local (small)	Single	0.5	0.58	0.05	0.092	9.8	36.5	1.3	38	1.1	0.98
LONG (wide)	Single	0.62	0.56	0.05	0.092	16.75	21.8	0.8	26	0.7	0.09
										Avg (f)	**0.20**
E-15	Dual	0.62	1.46	0.05	0.097	12.4	27.1	1.0	10	0.7	0.20

RESULTS											
Radiator	Pass	Inlet/outlet (in.)	Tube Width (in.)	Tube height (in.)	Dh (in.)	L (in.)	f	Area (Sq.in.)	Entry tubes	RF psi/gpm	RF (in. H2O/GPM)
E-15 Forecast	Dual	0.75	1.46	0.05	0.1	12.4	**0.2**	0.73	10	0.99	**27.4**
E-15 Actual	Dual	0.75	1.46	0.05	0.1	12.4	0.20	0.73	10	0.98	27.1

The average friction factor was calculated considering 4 tested radiators. The average friction factor as shown in Eqn 4-1 (a), then gives us resistance factor (RF) to forecast my design. From Figure 4-10, we can see that the RF value forecasted is almost equal to the actual design. Furthermore, the tested radiators are illustrated in a tabular format in figures C-1 to C-4 in Appendix C.

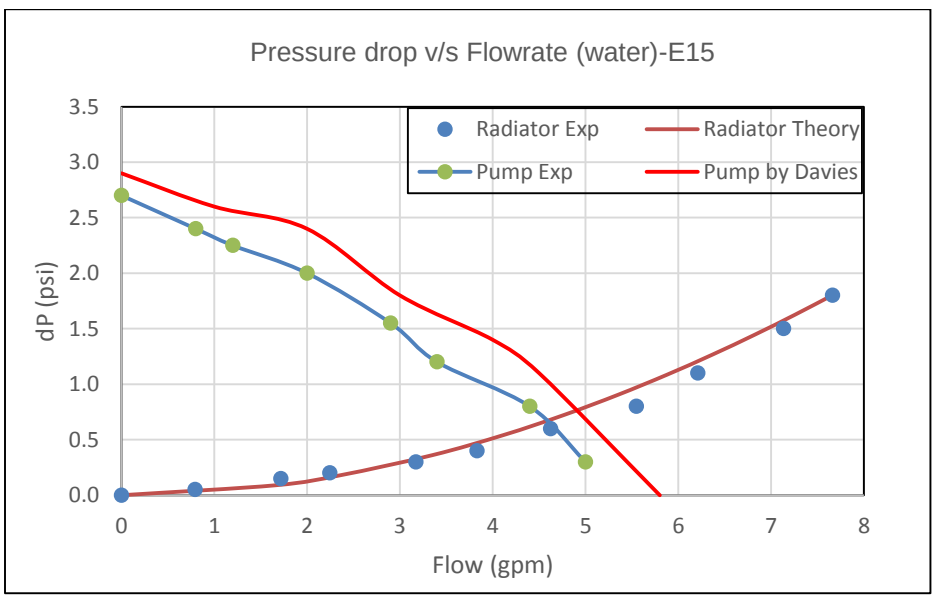

Figure 4-10 Water pressure test for radiator & pump

The selected pump was pressure tested similar to the flow test and the results have been extrapolated. The curve which shows pump experiment are actual results after testing it. The system and actual pump curve gives us the operating point for the actual flow.

Air pressure drop

<u>Radiators</u>

Figure 4-11 Radiators tested for system resistance curves

The system curve is developed very similar to the ones with water tests. The experimental setup and process shall be further explained. Equation 4-2 is used to formulate a theory which passes through all the experimental results.

Fig. 4-12 depicts system curves which are formulated and plotted similar to the ones for water test which are discussed as previous.

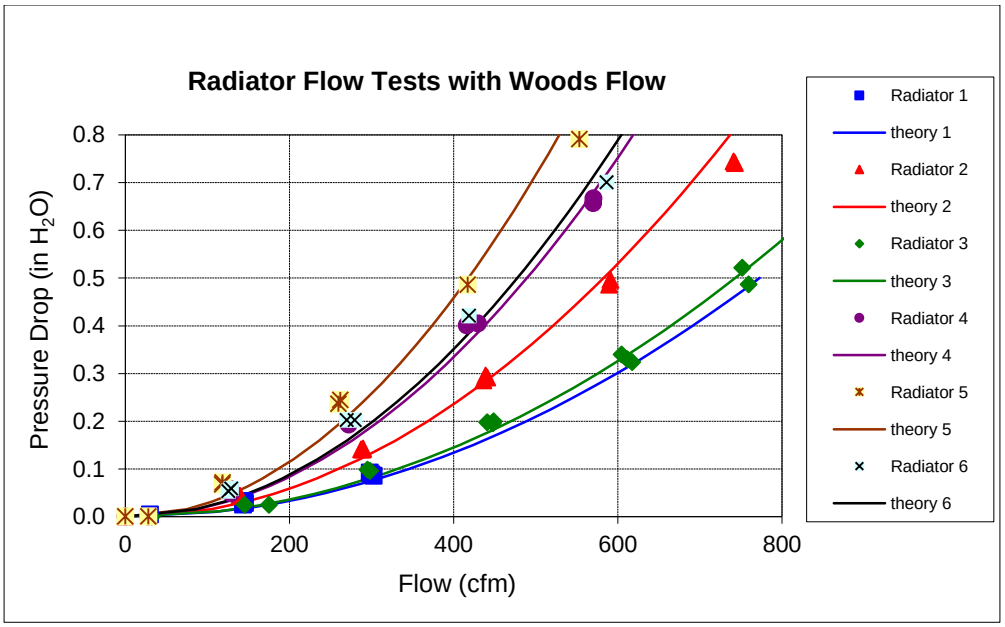

Figure 4-12 Tested radiators with system curves

E-15 Radiator

The current design was tested on the air flow bench with different variations. In this section we shall discuss the system resistance curve for the radiator only.

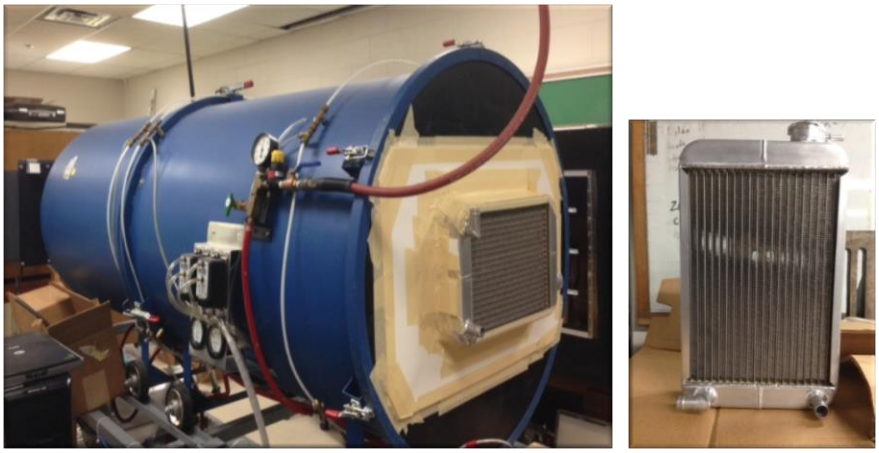

(a) (b)

Figure 4-13 (a) Radiator only tested on the air flow bench (b) Griffin E-15

The system curve is developed using the same equation for water resistance curves and the result is as shown below. Figure C-5 Appendix C illustrates the results in a tabular format.

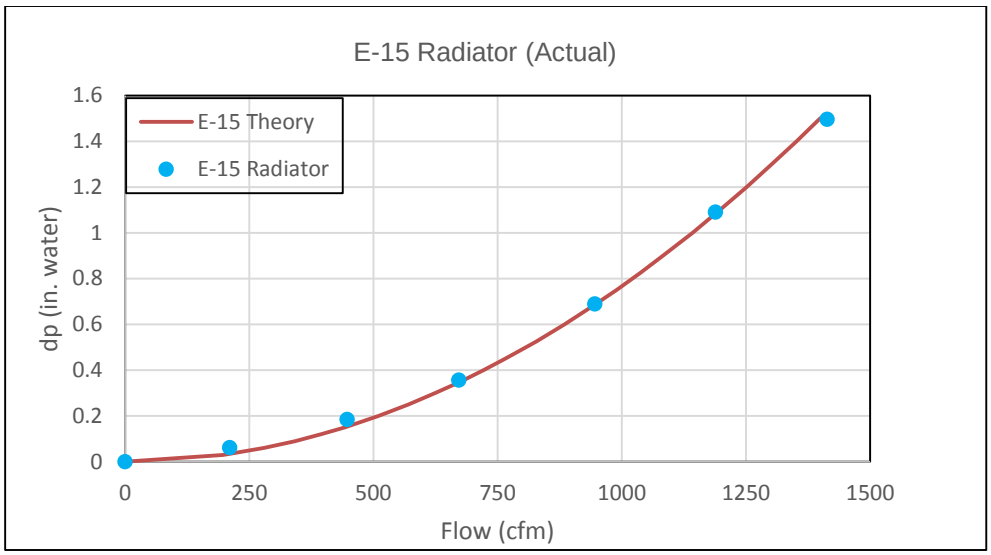

Figure 4-14 Radiator only tested & theory developed

<u>Fans</u>

Figure 4-15 Tripac and Spal fans tested for performance

The fans tested too are related to a theory which is a similar equation but not the same. It is indeed not easy to predict the theory of the same as the fan curve itself shows disturbed and random behaviors, depending on situations.

The equation that a fan follows is mentioned as below.

Fan curve theory,

$$\boxed{Q_{stc} = \frac{\left(\delta P_u - \delta P_{static}\right)}{RF}} \tag{4-2}$$

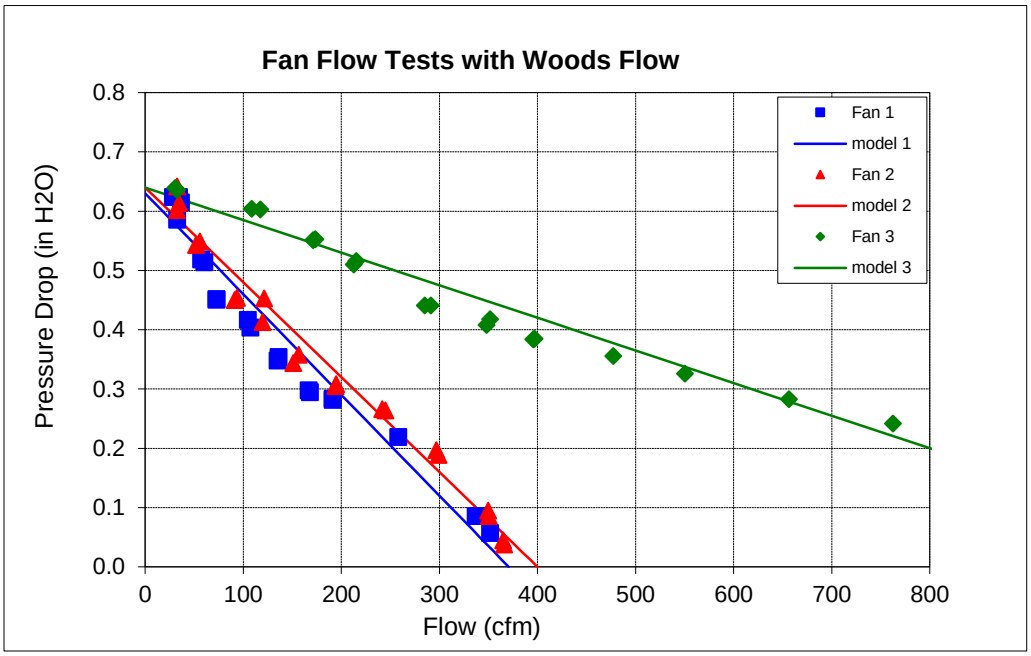

Figure 4-16 Tripac and Spal fan curves

Air flow summary

Table 4-2 Radiators tested & formulated RF factors

Radiators	length of H2O path (inches)	overall width (inches)	length of air path (inches)	overall area (inch^2)	width of each air row Wf (in)	number of air rows	fin density FD (fins/inch)	actual air flow width (in)	actual air flow area (in2)	RF (in H2O/cfm)	"L" (in)	"dh" (in)	friction factor f
1	10.25	11.75	1.250	120.4	0.380	25	15	9.50	90.1	0.026	1.250	0.112	0.48
2	13.00	8.88	1.915	115.4	0.380	19	18	7.22	85.4	0.034	1.915	0.096	0.41
3	10.25	11.75	1.250	120.4	0.380	25	15	9.50	90.1	0.027	1.250	0.112	0.51
4	9.10	9.00	2.000	81.9	0.375	19	13	7.13	60.6	0.041	2.000	0.125	0.38
5	11.75	7.50	1.250	88.1	0.375	15	17	5.63	60.5	0.048	1.250	0.101	0.66
6	15.00	6.00	1.250	90.0	0.375	13	19	4.88	66.2	0.042	1.250	0.092	0.55
F09	13.50	11.60	1.250	156.6	0.375	25	18	9.38	115.2	0.021	1.250	0.096	0.41
												Avg f =	**0.40**
E 15	12.4	9.4	1.5	**116.6**	**0.351**	**21**	**18**	**7.37**	**91.4**	**0.025**	**1.5**	**0.095**	**0.32**

RESULTS													
Radiators	length of H2O path (inches)	overall width (inches)	length of air path (inches)	overall area (inch^2)	Width air row Wf (in)	number of air rows	fin density FD (fins/inch)	actual air flow width (in)	actual air flow area (in2)	friction factor (Avg f)	"L" (in)	"dh" (in)	RF (in. H2O)/cfm
E15 Forecast	12.4	9.4	1.5	116.56	0.351	21	18	7.371	91.4	**0.40**	1.5	0.095	0.028
E15 Actual	12.4	9.4	1.5	116.56	0.351	21	18	7.371	91.4	**0.32**	1.5	0.095	**0.025**

As shown above the radiators tested are summarized in this Table which uses specific parameters in order to calculate frictional factors. The average taken from 3 radiators gives us a close friction factor to the actual one. The reason for selecting those 3 radiators were its length of air travel and variations in fin density.

Table 4-2 illustrates that the RF value as forecasted in almost similar to the actual value calculated. Hence it is a proven fact to judge future radiators on the basis of common frictional factors.

In the concluding part of this chapter we shall discuss more about system resistance and fan curves when assembled together as a radiator package which includes the assembly of a fan through a shroud.

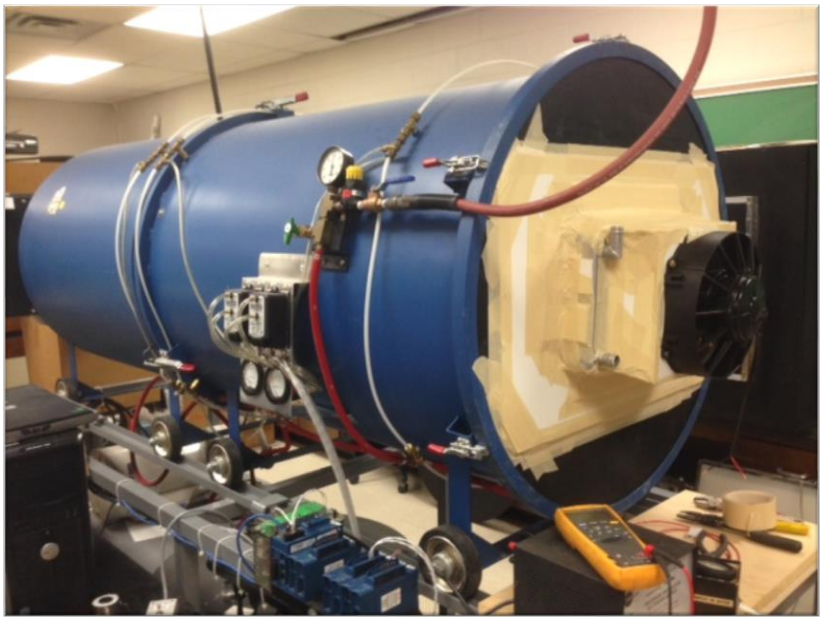

Figure 4-17 Fan & radiator with shroud

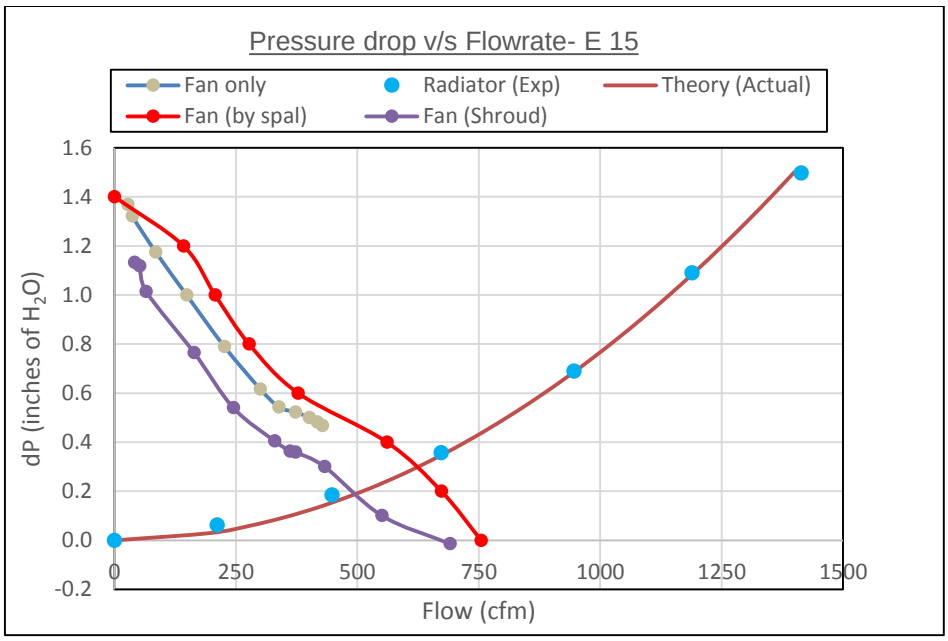

Figure 4-18 Operating point for fan only & fan with shroud

Figure 4-18 plays a vital role in predicting the actual flow rate of air through a system. Here, we can see that even the shroud provides a better cooling effect so does it decreases the fan's performance by shifting its zone of operation. This effect can be reduced if the outer edges are smoother which reduces eddy losses. The longer the shroud which means the fan's distance with the radiator core, better it is for the air flow. The main reason for the curve to act differently is the radiator which acts as further resistance to the air flow.

Table C-1 in Appendix C shows the results of all individual and shrouded assembly configurations. Another fact which many are misguided is the simple operation of amalgamating the system curve with the fan which is not true. A fan when assembled on a radiator along with or without a shroud, behaves differently which is observed in figure 4-18. Furthermore, if the fan is switched off then the system resistance results are shown below.

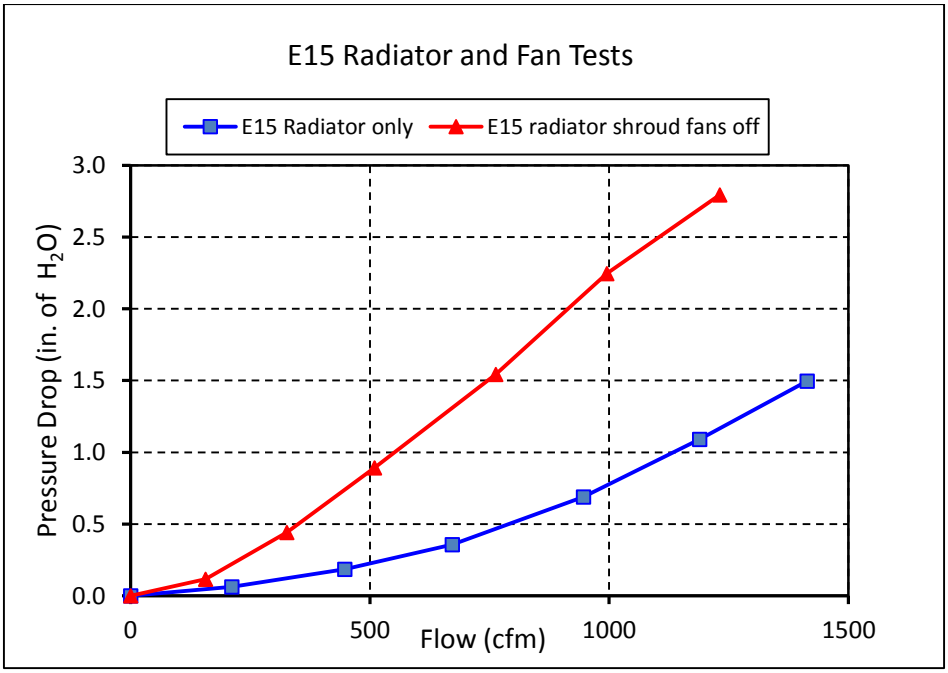

Figure 4-19 System curve change with fans off

Informatively, the larger the distance of the fan from it's system of focus, the better it is for the air flow as far as friction is concerned. In order to maintain your fan curve as best as what is given by the supplier, the shroud design too plays a vital role.

Fig. 4-19 depicts a difference in system resistances, i.e. an increase in resistance after having the complete package assembled with a non operating fan, but a blower that helps take readings. As components keep getting added, that itself becomes a system which generates more and more resistance.

In short, the same assembly has been tested with fans off, and the system curve slope changes significantly. This would never be a case in my application but a learning tool to understand the behavior of these curves with different arrangements.

Chapter 5

CONCLUSION

One can definitely conclude after this thesis, that with a given heat number to be rejected, we can obtain the correct pump and fan size appropriately that works effectively with the selected radiator size.

The fin efficiency along with thermal conduction has been neglected while using the NTU method for heat transfer from the radiator.

The pressure drop experimental values (radiators) are for an open system which possess greater losses such as velocity, pressure loss etc. as compared to only friction loss in a closed system.

According to the complete analysis, experiments and research carried out for the system, I conclude that my design and theory is applicable towards the pragmatic usage to develop or design heat exchanger systems, whether it be for automotive or commercial purposes.

Since the system has been applied to our existing electric car and will be used for combustion vehicles, it has been designed with a good amount of safety factor as it plays a vital role in avoiding switching off of the motors during endurance.

Although the pressure drop still needs the user to be well acquainted to the system and further have a sharp judgement in selecting radiators for average friction factors. It is applicable only to radiators with similar inlet/ outlet conditions.

This system indeed plays a vital role as far as cooling of electronics is concerned as higher the temperatures, greater is the impedance (resistance) of the system resulting in underperformance and depolarization.

Suggested future work for this thesis could be to use its data and theory for simulating it on ANSYS Icepak with relevant boundary conditions.

Appendix A

Average Power

Table A-1 Efficiency at different speeds

Motor Efficiencies						
Rear motor			**Front Motor**			**Motor**
Cont Efficiency	Peak Efficiency		Cont Efficiency	Peak Efficiency		Speed
(%)	(%)		(%)	(%)		(RPM)
0.83	0.73		0.78	0.64		1154
0.89	0.82		0.86	0.75		1978
0.92	0.86		0.89	0.81		2802
0.93	0.89		0.91	0.84		3626
0.94	0.91		0.93	0.87		4451
0.95	0.92		0.93	0.89		5275
0.95	0.93		0.94	0.9		6099
0.96	0.93		0.94	0.91		6923
0.96	0.94		0.95	0.91		7747
0.96	0.94		0.95	0.91		8571
0.96	0.94		0.95	0.91		9396
0.96	0.94		0.94	0.92		10220
0.95	0.94		0.94	0.92		11044
0.94	0.94		0.92	0.93		11868
0.92	0.94		0.9	0.92		12692
0.82	0.94		0.75	0.92		13516
0	0.94		0	0.91		14341
0	0.93		0	0.89		15000

Table A-2 Heat rejected at different speeds

DETERMINE TOTAL HEAT & SAFETY FACTOR								
Motor Speed	**Car Speed**	**Heat Produced**	**Total Rear Heat**	**Heat Produced**	**Total Front Heat**	**Total Heat**	**Safety Factor**	**Average**
(rpm)	(mph)	(Each Rear) %	(%)	(Each Front) %	(%)	(kW)	(SF)	(SF)
2802	13	13.7	27.3	19.2	38.3	6.0	2.1	1.4
3626	17	11.0	22.0	15.6	31.2	4.9	1.7	
4451	21	9.3	18.6	13.2	26.3	4.1	1.4	
5275	25	8.1	16.2	11.5	22.9	3.6	1.2	
6099	29	7.2	14.4	10.2	20.3	3.2	1.1	
6923	33	6.5	13.1	9.3	18.6	2.9	1.0	
6980	**33**	6.5	13.0	9.3	18.5	2.9	1.0	**Actual**
7747	37	6.2	12.4	8.9	17.8	2.8	1.0	
8571	41	6.1	12.1	8.7	17.4	2.7	0.9	
9396	44	6.0	12.0	8.6	17.2	2.7	0.9	
10220	48	6.0	12.1	7.9	15.8	2.6	0.9	
11044	52	6.1	12.2	7.5	15.0	2.6	0.9	
11868	56	6.1	12.2	7.4	14.8	2.5	0.9	
12692	60	6.0	12.1	7.5	15.0	2.5	0.9	
13516	64	6.1	12.3	8.0	15.9	2.6	0.9	
14341	68	6.4	12.8	9.1	18.1	2.8	1.0	
15000	71	6.8	13.5	11.1	22.2	3.2	1.1	
15863	75	7.3	14.7	14.7	29.4	3.8	1.3	

Appendix B

Heat Removal (NTU)

Table B-1 Air convective coefficients for 500 cfm

			For 500 CFM										
Tubes	H	L x H	Core Area		Free flow Area		Velocity	Char. Length		Reynolds	Pr	Nu	ha
	(in)	(Core)	(Sq. in)	(Sq. m)	(Sq. in)	(Sq. m)	(m/s)	(in)	(m)				(KW/m^2 deg C)
14	7	13.4 x 6.5	80.9	0.05	60.7	0.04	6.0	0.11	0.003	1139	0.7	20.0	0.19
16	8	13.4 x 7.4	91.8	0.06	68.7	0.04	5.3	0.11	0.003	1005	0.7	18.8	0.18
18	8	13.4 x 8.3	102.8	0.07	76.8	0.05	4.8	0.11	0.003	899	0.7	17.8	0.17
20	9	13.4 x 9.2	113.7	0.07	84.9	0.05	4.3	0.11	0.003	814	0.7	16.9	0.16
22	10	13.4 x 10.1	124.7	0.08	93.0	0.06	3.9	0.11	0.003	743	0.7	16.2	0.15
24	11	13.4 x 10.9	135.6	0.09	101.1	0.07	3.6	0.11	0.003	683	0.7	15.5	0.15
26	12	13.4 x 11.8	146.5	0.09	109.2	0.07	3.4	0.11	0.003	633	0.7	14.9	0.14
28	13	13.4 x 12.7	157.5	0.10	117.3	0.08	3.1	0.11	0.003	589	0.7	14.4	0.14

Table B-2 Water convective coefficients with outlet fluid temperatures

For 4 GPM																					
Tubes	Height	Min. Area	Vel.	Hyd. L	Re	Pr	Le(h)	Le(t)	f	Nu	hw	Fins	Aw	Aa	UA	NTU	Eff.	Qmax	Q	Tw (out)	Ta (out)
	(in)	(Sq. m)	(m/s)	(m)			(in)	(in)			(KW/m^2 deg C)		(Sq. m.)	(Sq. m.)			€	(KW)	(KW)	(deg C)	(deg C)
14	6.7	4.7E-05	0.8	0.002	3397	3.6			0.04	21.5	5.6	3300	0.34	2.60	0.39	1.3	0.67	8.4	5.6	52.6	48.7
16	7.6	4.7E-05	0.7	0.002	2972	3.6			0.05	18.3	4.8	3740	0.39	2.95	0.41	1.4	0.68	8.4	5.7	52.5	49.0
18	8.5	4.7E-05	0.6	0.002	2642	3.6			0.05	15.7	4.1	4180	0.43	3.31	0.42	1.4	0.69	8.4	5.8	52.4	49.3
20	9.4	4.7E-05	0.5	0.002	2378	3.6			0.05	13.5	3.5	4620	0.48	3.66	0.44	1.4	0.70	8.4	5.9	52.3	49.6
22	10.3	4.7E-05	0.5	0.002	2162	3.6	10.5	37.1		11.9	3.1	5060	0.53	4.01	0.45	1.5	0.71	8.4	6.0	52.3	49.8
24	11.1	4.7E-05	0.4	0.002	1982	3.6	9.6	34.0		11.7	3.1	5500	0.58	4.36	0.47	1.6	0.72	8.4	6.1	52.2	50.2
26	12.0	4.7E-05	0.4	0.002	1829	3.6	8.8	31.4		11.5	3.0	5940	0.63	4.71	0.49	1.6	0.74	8.4	6.2	52.1	50.6
28	12.9	4.7E-05	0.4	0.002	1699	3.6	8.2	29.2		11.3	3.0	6380	0.68	5.06	0.51	1.7	0.75	8.4	6.3	52.0	51.0

Other iterations too were calculated apart from 500 cfm and 4 gpm. This thesis covers a final selection of the above values which is why it is displayed. Further below the calculations for the same are shown along with the nomenclature.

Air properties are considered at 30 ºC and water at 50 ºC for the above fluid (convective) calculations.

NTU method nomenclature

n = Number of total tubes

N = Number of entering tubes

H = Radiator height

L = Radiator length

W_r (inner) = Radiator width, inner

W_r (outer) = Radiator width, outer

L_f = Fin length

W_f (inner) = Fin width, inner

W_f (outer) = Fin width, outer

H_f = Fin height

D = fin density

N_f = Number of fins per raw

n_f = Total number of fins

H_t (inner) = Tube height, inner

H_t (outer) = Tube height, outer

W_t (inner) = Tube width, inner

W_t (outer) = Tube width, outer

L_t= Tube length

$\dot{M}_w$ = Mass flow rate of water (kg/sec)

$\dot{M}_a$ = Mass flow rate of air (kg/sec)

Q (w) = Water flow rate (m^3/s)

Q (a) = Air flow rate (m^3/s)

μ_w = Dynamic viscosity of water

μ_a = Dynamic viscosity of air

v_w = Kinematic viscosity of water

v_a = Kinematic viscosity of air

ρ_w = Density of water (kg/m^3)

ρ_a = Density of air (Kg/m^3)

A_m = Minimum area of water flow per tube

A_c= Core area of radiator

A_f= Free flow area of radiator

V_w = Velocity of water (m/sec)

V_a = Velocity of air

A_w = Surface area exposed to water in the radiator (m^2)

A_a = Surface area exposed to air including fins (m^2)

P = Tube perimeter

D_h (w) = Hydraulic diameter of water

D_h (a) = Hydraulic diameter of air

C_p (w) = Specific heat of water at steady state temperature (kJ/kg ºC)

C_p (a) = Specific heat of air at steady state temperature (kJ/kg ºC)

T_w (i) = Temperature of hot water entering to the radiator (ºC)

T_w (o) = Temperature of cold water leaving the radiator (ºC)

T_a (i) = Temperature of cold air approaching the radiator (ºC)

T_a (o) = Temperature of hot air leaving the radiator (ºC)

Re_w = Reynolds number of water

Re_a = Reynolds number of air

Nu_w = Nusselt number of water

Nu_a = Nusselt number of air

Pr_w = Prandtl number of water

Pr_a = Prandtl number of air

h_w = Convective heat transfer coefficient of water inside the radiator (KW/m^2 deg C)

h_a = Convective heat transfer coefficient of air flowing over tubes (KW/m2 deg C)

K_w = Thermal conductivity of water

K_a = Thermal conductivity of air

$C_w = \dot{M}_w Cp_w$

$C_a = \dot{M}_a * Cp_a$

C_{min} = Min (C_w, C_a)

C_{max} = Max (C_w, C_a)

$C_r = C_{min} / C_{max}$)

UA = Overall heat transfer coefficient

NTU = Number of transfer unit

ε = Effectiveness of radiator

Q_{max} = Maximum possible heat transfer in radiator (kW)

Q = Net heat rejected from the radiator (kW)

The calculation for a combination of 20 tubes with 4 gpm and 500 cfm is illustrated as below.

N = 10

n = 20

H = 0.23876 m

L = 0.31496 m

W_r (inner) = 0.037 m

W_r (outer) = 0.038 m

L_f = 0.009 m

W_f (inner) = 0.037 m

W_f (outer) = 0.038 m

H_f = 0.0001 m

D = 18 / inch

N_f = 220

n_f = (n+1)* N_f = 4620

H_t (inner) = 0.001 m

H_t (outer) = 0.002 m

W_t (inner) = 0.037 m

W_t (outer) = 0.038 m

L_t = 0.31496 m

$\dot{M}_w$ = 4 gpm = 0.2493 kg/sec

$\dot{M}_a$ = 500 cfm = 0.298 kg/sec

Q (w) = 0.0002524 m^3/sec

Q (a) = 0.2360 m^3/sec

μ_w = 0.00055 Pa.sec

$\mu_a = 18.72 \times 10^{-6}$ (Pa sec)

$v_w = 0.553 \times 10^{-6}$ m^2 / sec

$v_a = 14.4*10^{-6}$ m^2 / sec

$K_w = 0.64$ W/ m ºC

$K_a = 26.49* 10^{-3}$ W / m ºC

$\rho_w = 988$ kg/ m^3

$\rho_a = 1.27$ kg/ m^3

$Cp_w = 4.18$ kJ/ kg ºC

$Cp_a = 1.01$ kJ/ kg ºC

T_w (i) = 55 ºC

T_a (i) = 30 ºC

$A_m = W_t$ (inner)* H_t (inner) = 5×10^{-5} m^2

$V_w = \frac{Q(w)}{N*Am} = 0.54$ m/sec

P = 2*(W_t (inner) + H_t (inner)) =0.076 m

D_h (w) = $\frac{4*Am}{P} = 0.0025$ m

$Re_w = \frac{Vw * \rho(w) * Dh\ (w)}{\mu\ (w)} = 2378$

$Pr_w = \frac{\mu\ (w)* Cp\ (w)}{K(w)} = 3.6$

FF = [1.58 ln (Re_w) – 3.28] $^{-2}$ = 0.12

Nu_w = [(Re_w –1000)*Pr_w*(FF/2)] / {1.07+ [(12.7 (FF/2)^{½} (Pr_w $^{2/3}$ - 1)]} = 13

$h_w = \frac{Nu\ (w)*K\ (w)}{Dh(w)} = 3.4$ kW/m^2 ºC

$A_w = 2\ n\ L_t$ (W_t (inner) + H_t (inner)) = 0.5 m^2

A_c= ((n*H_t) + ((n+1)*Lf))* L =0.07 m^2

A_f= Ac - ((N_f*(n+1))*L_f*H_f) + (n*H_t (outer)* L_t) = 0.06 m^2

$V_a = \frac{Q(a)}{Af}$ = 4.3 m/sec

$$D_h\ (a) = \frac{4*Am}{P} = \frac{4\left(\frac{\frac{2}{D}L(f)}{2}\right)}{\left(\frac{2}{D} + 2\sqrt{\left(\frac{1}{D}\right)^2 + W_f^2}\right)} = 0.003\ m$$

$Re_a = \frac{Vw * \rho(a) * Dh\ (a)}{\mu\ (a)}$ = 814

$Pr_a = \frac{\mu\ (a) * Cp\ (a)}{K(a)}$ = 0.7

Nu_a = 0.664 $Re_a^{0.5}$ $Pr_a^{0.33}$ = 16.9

$h_a = \frac{Nu\ (w) * K\ (w)}{Dh(w)}$ = 0.16 kW/m^2 ºC

A_a = (n 2 L_t (H_t (outer) + W_t (outer)) + (n_f 2 Lf (W_f (outer) + H_f)) = 3.7 m^2

$$UA = \frac{1}{\left(\frac{1}{h(a)*A\ (a)} + \frac{1}{h(w)*A\ (w)}\right)} = 0.43\ kW/\ ºC$$

C_w = $\dot{M}_w$ Cp_w = 1.04 kW/ ºC

C_a = $\dot{M}_a$ Cp_a = 0.30 kW/ ºC

C_{min} = Min (C_w, C_a) = 0.30 kW/ ºC

C_{max} = Max (C_w, C_a) = 1.04 kW/ ºC

$C_r = \frac{Cmin}{Cmax}$ = 0.29

$NTU = \frac{U*A}{Cmin}$ = 1.4

$\varepsilon = 1 - \exp\left(\frac{\exp\left(-Cr*NTU^{0.78}\right)-1}{Cr*NTU^{-0.22}}\right) = 0.7$

$Q_{max} = C_{min}$ (Tw (i) – Ta (i))= 7.5 kW

$Q = Q_{max}\ \varepsilon = 5.2$ kW

T_w (o) = $Tw\ (i) - \frac{Qmax}{Cw}$ = 50 ºC

T_a (o) = Temperature of hot air leaving the radiator = $Ta\ (i) - \frac{Qmax}{Ca}$ = 47.4 ºC

Appendix C

Pressure drop analysis

Griffin Radiator				
Flowmeter	Flow		Pr. Drop	
(%)	(LPM)	(GPM)	(Psi)	(in. H2O)
0	0	0	0	0
26.5	8	2.1	0.1	2.8
36.5	11	2.9	0.25	6.9
46.5	13.5	3.6	0.4	11.1
56.5	16.5	4.4	0.55	15.2
66.5	19.5	5.2	0.8	22.1
76.5	23.5	6.2	1	27.7
86.5	25.5	6.7	1.25	34.6
96.5	28	7.4	1.6	44.3
98.5	29	7.7	1.75	48.4

P(atm) = 29.92 in Hg
RF = 26.7 in H2O/GPM

49		
DPstatic		Flow
(in H2O)		(GPM)
0		0.0
2.5		1.7
4.9		2.4
9.8		3.4
14.7		4.1
19.6		4.8
24.5		5.4
29.4		5.9
34.3		6.4
39.2		6.9
44.1		7.3
49.0		7.7

(a) (b) (c)

Figure C-1 (water) (a) Experimental results (b) Theory (c) Griffin dual pass

F-09 Radiator (LONG)				
Flowmeter	Flow		Pr. Drop	
(%)	(LPM)	(GPM)	(Psi)	(in H2O)
0	0	0	0	0
26.5	8	2.1	0.25	6.9
36.5	11	2.9	0.35	9.7
46.5	13.5	3.6	0.45	12.5
56.5	16.5	4.4	0.55	15.2
66.5	19.5	5.2	0.67	18.5
76.5	23.5	6.2	0.8	22.1
86.5	25.5	6.7	1.10	30.4
96.5	28	7.4	1.38	38.2
98.5	29	7.7	1.5	41.5

P(atm) = 29.92 in Hg
RF = 24.4 in H2O/GPM

42		
DPstatic		Flow
(in H2O)		(GPM)
0		0.0
2.1		1.7
4.2		2.4
6.3		2.9
8.4		3.4
10.5		3.8
13.3		4.3
16.1		4.7
18.9		5.1
21.7		5.5
25.9		6.0
30.1		6.5
34.3		7.0
38.5		7.4
42.7		7.8

(a) (b) (c)

Figure C-2 (water) (a) Experimental results (b) Theory (c) F-09 dual pass

LONG Radiator (Woods)				
Flowmeter	Flow		Pr. Drop	
(%)	(LPM)	(GPM)	(Psi)	(in H2O)
0	0	0	0	0
26.5	8	2.1	0.1	2.8
36.5	11	2.9	0.15	4.2
46.5	13.5	3.6	0.2	5.5
56.5	16.5	4.4	0.25	6.9
66.5	19.5	5.2	0.4	11.1
76.5	23.5	6.2	0.47	13.0
86.5	25.5	6.7	0.55	15.2
96.5	28	7.4	0.7	19.4
98.5	29	7.7	0.75	20.8

(a)

P(atm) = 29.92 in Hg
RF = 17.4 in H2O/GPM
21

DPstatic (in H2O)		Flow (GPM)	
0		0.0	
1.1		1.7	
2.1		2.4	
3.2		2.9	
4.2		3.4	
5.6		3.9	
7.0		4.4	
8.4		4.8	
9.8		5.2	
11.9		5.7	
14.0		6.2	
16.1		6.6	
18.2		7.075	
20.3		7.481	
22.4		7.869	

(b)

(c)

Figure C-3 (water) (a) Experimental results (b) Theory (c) LONG single pass

LONG Radiator (wide)				
Flowmeter	Flow		Pr. Drop	
(%)	(LPM)	(GPM)	(Psi)	(in H2O)
0	0	0	0	0
26.5	8	2.1	0.1	2.8
36.5	11	2.9	0.2	5.5
46.5	13.5	3.6	0.3	8.3
56.5	16.5	4.4	0.4	11.1
66.5	19.5	5.2	0.5	13.8
76.5	23.5	6.2	0.7	19.4
86.5	25.5	6.7	0.80	22.1
96.5	28	7.4	1.1	30.4
98.5	29	7.7	1.2	33.2

(a)

P(atm) = 29.92 in Hg
RF = 21.8 in H2O/GPM
34

DPstatic (in H2O)		Flow (GPM)
0		0.0
1.7		1.7
3.4		2.4
5.1		3.0
6.8		3.4
8.5		3.8
10.2		4.2
11.9		4.5
15.3		5.2
18.7		5.7
22.1		6.2
25.5		6.7
28.9		7.2
32.3		7.6
35.7		8.0

(b)

(c)

Figure C-4 (water) (a) Experimental results (b) Theory (c) LONG single pass (wide)

MY DESIGN				
Griffin (E-15) Radiator				
Flowmeter	Flow		Pr. Drop	
(%)	(LPM)	(GPM)	(Psi)	(in. H2O)
0	0	0	0.0	0
10	3	0.8	0.1	1.4
20	6.5	1.7	0.2	4.2
30	8.5	2.2	0.2	5.5
40	12	3.2	0.3	8.3
50	14.5	3.8	0.4	11.1
60	17.5	4.6	0.6	16.6
70	21	5.5	0.8	22.1
80	23.5	6.2	1.1	30.4
90	27	7.1	1.5	41.5
100	29	7.7	1.8	49.8

(a)

P(atm) = 29.92 in Hg
RF = 27.1 in H2O/GPM
50

DP static		Flow
(in H2O)	psi	(GPM)
0	0	0.0
2.5	0.1	1.7
5.0	0.2	2.4
10.0	0.4	3.4
15.0	0.5	4.1
20.0	0.7	4.8
25.0	0.9	5.3
30.0	1.1	5.9
35.0	1.3	6.4
40.0	1.4	6.8
45.0	1.6	7.3
50.0	1.8	7.7

(b)

(c)

Figure C-5 (water) (a) Experimental results (b) Theory (c) E-15 Griffin tested

Radiator E-15 (Theory)	
Patm = 29.92 in Hg	
RF = 0.025 in H2O/cfm	
1.5	
DPstatic (in H2O)	Flow (cfm)
0	0.0
0.030	197.7
0.060	279.6
0.090	342.5
0.120	395.5
0.150	442.2
0.200	510.6
0.250	570.9
0.300	625.4
0.350	675.5
0.400	722.2
0.450	766.0
0.525	827.4
0.600	884.6
0.675	938.3
0.750	989.1
0.825	1037
0.900	1084
1.000	1142
1.100	1198
1.200	1251
1.300	1303
1.400	1352
1.500	1399

(a)

Pbaro = 29.92 in Hg

Radiator E-15 (Exp)				
DPflow (in H2O)	Pup (psi)	Nw	Flow (cfm)	DPstatic (in H2O)
0	14.694	0	0	0
0.059	14.698	0.000	211.3	0.062
0.260	14.710	0.001	447.6	0.185
0.586	14.728	0.002	672.3	0.357
1.164	14.761	0.005	946.1	0.689
1.843	14.800	0.008	1189.2	1.090
2.613	14.842	0.011	1413.8	1.497

(b)

Figure C-6 (air) (a) Experimental results (b) Theory for E-15 radiator

Table C-1 Fan tested with radiator individually and shrouded assembly

test condition	raw signal DP_{flow} (volts)	raw signal DP_{load} (volts)	DP_{flow} (in H_2O)	DP_{load} (in H_2O)	Pup (psi)	ρ (lbm/ft^3)	N_w (-)	C_d (-)	Flow (cfm)
E15 Radiator only									
0	0.004	0.008	0.000	0.000	14.69	0.0746	0.0000	0.940	0
10	0.062	0.039	0.059	0.062	14.70	0.0746	0.0120	0.979	211
20	0.264	0.100	0.260	0.185	14.71	0.0746	0.0253	0.986	448
30	0.590	0.187	0.586	0.357	14.73	0.0747	0.0380	0.986	672
40	1.167	0.353	1.164	0.689	14.76	0.0749	0.0536	0.986	946
50	1.847	0.553	1.843	1.090	14.80	0.0751	0.0676	0.986	1189
60	2.616	0.756	2.613	1.497	14.84	0.0753	0.0806	0.986	1414
E15 Fan only									
zero	0.004	0.008	0.000	0.000	14.69	0.0746	0.0000	0.940	0
open	0.241	0.242	0.238	0.468	14.72	0.0747	0.0242	0.985	428
closing 1	0.230	0.249	0.226	0.482	14.72	0.0747	0.0236	0.985	417
closing 2	0.213	0.259	0.209	0.501	14.72	0.0747	0.0227	0.985	401
closing 3	0.184	0.269	0.181	0.522	14.72	0.0747	0.0211	0.985	373
closing 4	0.153	0.280	0.149	0.544	14.72	0.0747	0.0192	0.984	338
closing 5	0.121	0.316	0.117	0.617	14.72	0.0747	0.0170	0.983	300
closing 6	0.071	0.403	0.067	0.790	14.72	0.0747	0.0129	0.980	226
closing 7	0.033	0.508	0.029	1.000	14.73	0.0748	0.0085	0.974	148
closing 8	0.013	0.595	0.010	1.175	14.74	0.0748	0.0049	0.965	85
closing 9	0.005	0.669	0.002	1.321	14.74	0.0748	0.0021	0.953	37
closing 10	0.005	0.693	0.001	1.369	14.74	0.0748	0.0016	0.950	28
E15 radiator shroud fan on									
zero	0.003	0.008	0.000	0.000	14.69	0.0746	0.0000	0.940	0
boost 40	0.197	0.198	0.194	0.380	14.71	0.0747	0.0219	0.985	386
boost 20	0.194	0.197	0.191	0.379	14.71	0.0747	0.0217	0.985	383
boost 10	0.193	0.197	0.190	0.378	14.71	0.0747	0.0216	0.985	382
full open	0.190	0.192	0.187	0.368	14.71	0.0747	0.0215	0.985	379
closing 1	0.176	0.198	0.173	0.381	14.71	0.0747	0.0207	0.985	365
closing 2	0.145	0.216	0.142	0.416	14.71	0.0747	0.0187	0.984	330
closing 3	0.113	0.243	0.110	0.471	14.71	0.0747	0.0165	0.983	290
closing 4	0.078	0.305	0.075	0.595	14.72	0.0747	0.0136	0.981	239
closing 5	0.046	0.372	0.043	0.729	14.72	0.0747	0.0103	0.977	181
closing 6	0.018	0.466	0.015	0.916	14.73	0.0747	0.0061	0.968	106
closing 7	0.009	0.540	0.005	1.065	14.73	0.0748	0.0036	0.960	62
closing 8	0.008	0.573	0.004	1.130	14.73	0.0748	0.0033	0.959	57
closing 9	0.008	0.572	0.004	1.129	14.73	0.0748	0.0033	0.959	57
E15 radiator shroud fans on boost									
zero	0.003	0.008	0.000	0.000	14.69	0.0746	0.0000	0.940	0
open boost 30	0.622	0.001	0.618	-0.014	14.72	0.0747	0.0390	0.986	691
open boost 20	0.396	0.059	0.392	0.101	14.71	0.0747	0.0311	0.986	550
open boost 10	0.246	0.158	0.243	0.300	14.71	0.0747	0.0245	0.985	432
full open	0.184	0.188	0.180	0.359	14.71	0.0747	0.0211	0.985	372
closing 1	0.173	0.189	0.170	0.363	14.71	0.0747	0.0205	0.985	361
closing 2	0.145	0.210	0.142	0.405	14.71	0.0747	0.0187	0.984	330
closing 3	0.082	0.278	0.078	0.540	14.72	0.0747	0.0139	0.981	245
closing 4	0.039	0.391	0.036	0.765	14.72	0.0747	0.0094	0.975	164
closing 5	0.009	0.515	0.006	1.014	14.73	0.0748	0.0038	0.961	65
closing 6	0.007	0.567	0.004	1.119	14.73	0.0748	0.0030	0.957	52
closed	0.006	0.574	0.002	1.132	14.73	0.0748	0.0024	0.954	41

References

1. Images used in this thesis mentioned as representation only are credits to www.google.com
2. FSAE 2015 rule book
3. http://engineering.lamar.edu/_files/documents/mechanical/dr.-fan-publications/2012/No%2031%202012%20ASEE%20Radiator%20Final.pdf for Nusselt relation of air.
4. http://iosrjournals.org/iosr-jmce/papers/RDME-Volume2/RDME-11.pdf for heat transfer (NTU)
5. Heat conduction through fins by Prabal Talukdar (IIT Delhi)
6. Designing a more effective car radiator by Maplesoft for convective coefficients, hydraulic diameters and heat transfer.
7. Online thermal properties considered for fluids (water and air) from peace software
8. Websites for davies craig (water pump) , Spal for fan and Griffin custom radiators for a dual pass radiator.
9. Credits for equations 3-5, 4-1 (a), (b) and (c) purely go to Dr. Robert Woods
10. http://web2.clarkson.edu/projects/subramanian/ch330/notes/Heat%20Transfer%20in%20Flow%20Through%20Conduits.pdf for thermal and hydraulic boundary layer considerations.
11. Handbook of heat transfer- Mcgraw Hill 3rd edition
12. Convective heat transfer- Michel Favre Marinet Sedat Tardu
13. Heat transfer principles in Electronics cooling- Part B chapter 9.
14. Thermal development of internal flows – P M V Subbarao (IIT Delhi)
15. Internal flow- Heat transfer correlations, chapter 8 sections 8.4 through 8.8

Biographical Information

As far as Shahzad's past academics are concerned, he has completed diploma in mechanical engineering with two major internships in automotive and aircraft industries. Further ahead, after completing his bachelors in mechanical engineering, he does believe that an engineer should always be aquainted to management knowledge, which is why he decided to earn a degree in management with operations as a specialization. During MBA studies, he takes pride in designing/ modulating an automated welding machine during his internship with a refrigeration company which reflected productive results. The above all stated was his education and experience in India.

He has currently earned a degree from The University of Texas at Arlington in mechanical engineering as a graduate student and moreover takes pride in being a part of the University's Formula SAE race team which is a well known student body competition, and further helps one in creating an identity as a role model for leading a racecar subsystem. Formula SAE at UTA has indeed provided him with that knowledge, professionalism, expertise and moreover an identity to prove oneself worthy enough to be employed.

This thesis opportunity has helped him gain immense knowledge which further inspires to grow and research more in the HVAC/ thermal systems sector. He is also inclined towards green technology, which is why he decided to take up this project, which further enables him to be employed within the electric car industry. Tesla motors being one of his dream companies has always been a sense of inspiration towards technological growth, as well as their policy of continuous innovation drives an engineer to believe in unrealistic possibilities.